

Journal of African Earth Sciences

The influence of taphonomy and time on the paleobotanical record of the Permian–Triassic transition of the Karoo Basin (and elsewhere)

--Manuscript Draft--

Manuscript Number:	
Article Type:	VSI: Legacy Africa Review Paper
Keywords:	plant taphonomy, paleobotany, palynology, end-Permian event, geochronology, magnetostratigraphy
Corresponding Author:	Robert A Gastaldo, Ph.D Colby College Waterville, ME UNITED STATES
First Author:	Robert A Gastaldo, Ph.D
Order of Authors:	Robert A Gastaldo, Ph.D Marion Bamford
Abstract:	<p>Terrestrial assemblages preserved in the upper Permian–lower Triassic strata of the Karoo Basin, South Africa, have played a central role in the interpretation of ecosystem patterns. However, these models need to be carefully reconsidered because of the limitations of the rock record. Four lessons learned from a more robust approach to the rocks, lithology, continental sequence stratigraphy, and dating are relevant to other paleofloras in large terrestrial basins. In reality, the Karoo paleofloral record is very sparse. Hence, reports of a near continuous fossil record in this basin should be considered as the near continuous record of erosion and time lost with sporadic phytoclast fields.</p> <p>A review of the debate over the rate and timing of the end Permian extinction as represented in the Karoo Basin reinforces the need for extensive stratigraphic mapping, the depositional environment of the plants, as well as the application of a variety of dating methods. First, the Karoo late Permian to early Triassic paleobotanical assemblages are extremely rare with only a handful of sites in the Free State and Eastern Cape Provinces. These data originate from >3750 m of total measured section wherein megafloral remains are preserved in < 1% of the available rock record (0.9% all megafloral elements; permineralized wood = 0.1%, adpressions = 0.8 %), with spore-and-pollen assemblages only slightly more frequently encountered at 1.3%. This low occurrence is comparable with other basins. Thus, any continental fossil assemblage represents a very short temporal window into the paleobiosphere because of taphonomic effects of the soils, pedogenesis, and controls on depositional environments. Second, geochronometric and rock magnetic data, developed in a sequence stratigraphic context, are critical to constrain time and biological trends in continental successions. The missing time, diatems and hiatuses, are critically important. Third, the spatial relationships of plant-fossil assemblages are not easily correlated across the basin without an extensive dataset of the landscape. In general, the late Permian Beaufort rocks represent channels, floodplains, and braided streams rather than lakes and oxbows conducive to the preservation of phytoclasts. Finally, the temporal distribution of paleobotanical assemblages is complicated by the missing time (sediments) that has resulted in the apparent scarcity of vegetation before and after the end Permian extinction. Uncharacteristic diversity and abundance of plants in the Carnian–Norian Molteno Formation is most likely due to an environment conducive to preserving paleobotanical assemblages as well as a record of intensive collecting. Overall, the large inland Karoo Basin, without any marine influence or extensive volcanic deposits, has favored the preservation of vertebrate assemblages here and in other terrestrial basins.</p>
Suggested Reviewers:	Joerg Schneider Joerg.Schneider@geo.tu-freiberg.de Committee member of the Commission on Permian Stratigraphy; continental stratigraphy and paleontology
	Elke Schneebeli-Hermann elke.schneebeli@pim.uzh.ch

	Permian--Triassic paleobotanistpalynologist with expertise in paleoecology
	Steve Holland stratum@uga.edu Steve Holland, better known for his studies in marine sequence stratigraphy, has recently applied his focus on terrestrial settings in which plant fossils may accumulate. His working knowledge of taphonomy, stratigraphy, and the paleontological record makes him ideal for reviewing this manuscript. Also, his recent co-author--Anik K. Regan (listed in the cover letter)--has focused on the continental plant-fossil record.
	Steffen Trümper steffen.truemper@hotmail.de In collaboration with Ronnie Roessler, Chemnitz, Steffen has been focused on Permian fossil-plant taphonomy, depositional environments, and paleoecology in central Europe.

Prof. Barbara J. Tewksbury
Hamilton College
198 College Hill Rd.
Clinton, NY 13323

December 5, 2022

Dear Barbara and guest co-editors

Please find our invited contribution to the special volume of the Journal of African Earth Sciences focused on the paleobotanical record spanning the latest Permian and earliest Triassic interval in the Karoo Basin. The manuscript is a collaborative effort with Prof. Marion Bamford, and is entitled “The influence of taphonomy and time on the paleobotanical record of the Permian–Triassic transition of the Karoo Basin (and elsewhere).” As per your request and instructions, we have taken a “Lessons” approach to our manuscript, incorporating a multidisciplinary data set that our colleagues and ourselves have amassed over the past 20 years in the basin. We understand that the intent of the special issue is to review our current state-of-knowledge on the topic, which we have done. To provide the community with the necessary insights into how our work applies not only to the Karoo basin, but to any (and all) fully terrestrial settings, we have included several new analyses of the plant-fossil record in the succession, how that record parses in time (as determined via geochronology and magnetostratigraphy) and space (distribution of potential depositional environments), and provided reasons and rationale as to why megafloral assemblages are a rarity. Where appropriate, we compare our Karoo data with a similar data set from the Hami-Turpan Basin, western China (Gastaldo et al., in press, PALAIOS), demonstrating that our results are cosmopolitan and our conclusions applicable elsewhere. None of our analytical Karoo-Basin results have (or will) appear elsewhere; of course, much of our contextual data appear in a number of our previous publications.

Due to the mixed nature of a review article and the presentation of new analyses, we suggest the following colleagues who have demonstrable expertise in the array of topics and methodologies discussed in our manuscript.

- Prof. Jörg Schneider, TU Bergakademie Freiberg, Department of Palaeontology and Stratigraphy, D-09596 Freiberg, Germany; Joerg.Schneider@geo.tu-freiberg.de
- Dr. Elke Schneeblei-Hermann, Paläontologisches Institut und Museum, 8006 Zürich, Switzerland; elke.schneeblei@pim.uzh.ch
- Prof. Steve Holland, Department of Geology, University of Georgia, Athens, GA 30602-2501, stratum@uga.edu
- Dr. Spencer Lucas, The New Mexico Museum of Natural History & Science, Albuquerque, NM, 87104; spencer.lucas@state.nm.us
- Dr. Steffen Trümper, Museum für Naturkunde Chemnitz, 09111 Chemnitz, Germany; steffen.truemper@hotmail.de
- Prof. Dr. Hans Kerp, Institute of Geology and Palaeontology – Palaeobotany, University of Münster, D-48149 Münster, Germany; kerp@uni-muenster.de
- Dr. Garland Upchurch, Curator Adjoint, University of Colorado Boulder, Museum of Natural History, Boulder, CO 80309; garland.upchurch@colorado.edu
- Dr. Anik K. Regan, Department of Earth, Environment, and Society, University of St. Thomas, Saint Paul, MN 55105-1096; rega6944@stthomas.edu

We look forward to learning of the reviewer’s suggestions and comments, and a decision on our contribution after the New Year. We appreciate having been offered this opportunity to contribute to the Legacy volume.

Best Regards,

Bob

ABSTRACT

Terrestrial assemblages preserved in the upper Permian–lower Triassic strata of the Karoo Basin, South Africa, have played a central role in the interpretation of ecosystem patterns. However, these models need to be carefully reconsidered because of the limitations of the rock record. Four lessons learned from a more robust approach to the rocks, lithology, continental sequence stratigraphy, and dating are relevant to other paleofloras in large terrestrial basins. In reality, the Karoo paleofloral record is very sparse. Hence, reports of a near continuous fossil record in this basin should be considered as the near continuous record of erosion and time lost with sporadic phytoclast fields.

A review of the debate over the rate and timing of the end Permian extinction as represented in the Karoo Basin reinforces the need for extensive stratigraphic mapping, the depositional environment of the plants, as well as the application of a variety of dating methods. First, the Karoo late Permian to early Triassic paleobotanical assemblages are extremely rare with only a handful of sites in the Free State and Eastern Cape Provinces. These data originate from >3750 m of total measured section wherein megafloral remains are preserved in < 1% of the available rock record (0.9% all megafloral elements; permineralized wood = 0.1%, adpressions = 0.8 %), with spore-and-pollen assemblages only slightly more frequently encountered at 1.3%.

This low occurrence is comparable with other basins. Thus, any continental fossil assemblage represents a very short temporal window into the paleobiosphere because of taphonomic effects of the soils, pedogenesis, and controls on depositional environments. Second, geochronometric and rock magnetic data, developed in a sequence stratigraphic context, are critical to constrain time and biological trends in continental successions. The missing time, diatems and hiatuses, are critically important. Third, the spatial relationships of plant–fossil assemblages are not easily correlated across the basin without an extensive dataset of the landscape. In general, the late Permian Beaufort rocks represent channels, floodplains, and braided streams rather than lakes and oxbows conducive to the preservation of phytoclasts. Finally, the temporal distribution of paleobotanical assemblages is complicated by the missing time (sediments) that has resulted in the apparent scarcity of vegetation before and after the end Permian extinction. Uncharacteristic diversity and abundance of plants in the Carnian–Norian Molteno Formation is most likely due to an environment conducive to preserving paleobotanical assemblages as well as a record of intensive collecting. Overall, the large inland Karoo Basin, without any marine influence or extensive volcanic deposits, has favored the preservation of vertebrate assemblages here and in other terrestrial basins.

Highlights

We present four lessons learned about the fossil-plant assemblages in the Karoo Basin, spanning the late Permian–early Triassic, that should be applied in other, fully continental settings regardless of age. The first lesson focuses on the proportional representation of the stratigraphic study interval, consisting of >3750 m of measured section. Here, fossiliferous horizons encountered account for <1% for megaflooras and <1/5% for microflooras. The second lesson concerns the paradigm of “continuous” continental records across this interval. The Karoo succession is not continuous, even when the presence of minor temporal diastems or hiatuses in paleosols are acknowledged. Time is constrained best when using both geochronology and rock magnetic properties (i.e., magnetostratigraphy) in the absence of U-Pb datable minerals. Thirdly, Plant-fossil assemblages are neither distributed equally within or across correlative sections. Our understanding of vegetation in this part of the Karoo succession is contingent on a limited number of fossiliferous beds that, generally, are preserved over a rock thickness of a few decimeters, and are restricted in available outcrops. Lastly, the frequency of plant-bearing beds over a stratigraphic interval of interest will dictate one’s perception of biological trends in time. This is because each assemblage represents a very short temporal “window” into the (paleo)biosphere, providing snapshots with which to connect-the-dots and discern biological patterns.

[Click here to view linked References](#)

1
2
3
4 The influence of taphonomy and time on the paleobotanical record of the Permian–Triassic
5 transition of the Karoo Basin (and elsewhere)
6

7
8 Robert A. Gastaldo¹

9 Department of Geology, Colby College, Waterville, ME 04901 USA

10 and

11 Marion K. Bamford

12 Evolutionary Studies Institute, University of Witwatersrand, 1 Jan Smuts Avenue, Braamfontein
13 2000, Johannesburg, South Africa
14
15

16
17 ¹Corresponding Author email: ragastal@colby.edu
18

19 **1 ABSTRACT**

20
21
22 2 Terrestrial assemblages preserved in the upper Permian–lower Triassic strata of the Karoo Basin,
23
24 3 South Africa, have played a central role in the interpretation of ecosystem patterns. However,
25
26
27 4 these models need to be carefully reconsidered because of the limitations of the rock record. Four
28
29 5 lessons learned from a more robust approach to the rocks, lithology, continental sequence
30
31 stratigraphy, and dating are relevant to other paleofloras in large terrestrial basins. In reality, the
32 6 Karoo paleofloral record is very sparse. Hence, reports of a near continuous fossil record in this
33
34 7 basin should be considered as the near continuous record of erosion and time lost with sporadic
35
36
37 8 phytoclast fields.
38
39 9

40
41
42 10 A review of the debate over the rate and timing of the end Permian extinction as
43
44 11 represented in the Karoo Basin reinforces the need for extensive stratigraphic mapping, the
45
46
47 12 depositional environment of the plants, as well as the application of a variety of dating methods.
48
49 13 First, the Karoo late Permian to early Triassic paleobotanical assemblages are extremely rare
50
51
52 14 with only a handful of sites in the Free State and Eastern Cape Provinces. These data originate
53
54 15 from >3750 m of total measured section wherein megafloral remains are preserved in < 1% of
55
56
57 16 the available rock record (0.9% all megafloral elements; permineralized wood = 0.1%,
58
59 17 adpressions = 0.8 %), with spore-and-pollen assemblages only slightly more frequently
60
61
62
63
64
65

1
2
3
4 18 encountered at 1.3%. This low occurrence is comparable with other basins. Thus, any continental
5
6
7 19 fossil assemblage represents a very short temporal window into the paleobiosphere because of
8
9 20 taphonomic effects of the soils, pedogenesis, and controls on depositional environments. Second,
10
11
12 21 geochronometric and rock magnetic data, developed in a sequence stratigraphic context, are
13
14 22 critical to constrain time and biological trends in continental successions. The missing time,
15
16
17 23 diatems and hiatuses, are critically important. Third, the spatial relationships of plant-fossil
18
19 24 assemblages are not easily correlated across the basin without an extensive dataset of the
20
21
22 25 landscape. In general, the late Permian Beaufort rocks represent channels, floodplains, and
23
24 26 braided streams rather than lakes and oxbows conducive to the preservation of phytoclasts.
25
26
27 27 Finally, the temporal distribution of paleobotanical assemblages is complicated by the missing
28
29 28 time (sediments) that has resulted in the apparent scarcity of vegetation before and after the end
30
31
32 29 Permian extinction. Uncharacteristic diversity and abundance of plants in the Carnian–Norian
33
34 30 Molteno Formation is most likely due to an environment conducive to preserving paleobotanical
35
36
37 31 assemblages as well as a record of intensive collecting. Overall, the large inland Karoo Basin,
38
39 32 without any marine influence or extensive volcanic deposits, has favored the preservation of
40
41
42 33 vertebrate assemblages here and in other terrestrial basins.

43
44 34 Keywords: plant taphonomy, paleobotany, palynology, end-Permian event, geochronology,
45
46
47 35 magnetostratigraphy
48
49
50
51
52
53
54
55
56
57
58
59
60
61
62
63
64
65

1
2
3
4 36 **1. Introduction**
5
6

7 37 Terrestrial assemblages preserved in the upper Permian–lower Triassic strata of the Karoo
8
9 38 Basin, South Africa, have played a central role in the interpretation of ecosystem patterns (e.g.,
10
11
12 39 Smith and Botha-Brink, 2014) and modeled terrestrial dynamics (e.g., Angielczyk et al., 2005;
13
14 40 Roopnarine et al., 2019) related to the end-Permian crisis. The reported extinction-and-
15
16
17 41 replacement of vertebrates, used to interpret a short-term, mass-extinction event over a very thin
18
19 42 stratigraphic interval (e.g., Viglietti et al., 2021), is predicated on a hypothesis about the
20
21
22 43 catastrophic demise of a landscape forested and dominated by *Glossopteris* taxa (e.g., Retallack
23
24 44 et al., 2003; Ward et al., 2005). Glossopterid vegetation is thought to have been “replaced”
25
26
27 45 rapidly, first, by equisetalean and, then, lycopsid and other gymnosperm taxa which were adapted
28
29 46 to climatically stressed conditions. Arid and semi-arid conditions are interpreted to have
30
31
32 47 prevailed into the Upper Triassic (~Carnian; Bordy et al., 2020) before seasonally warm and
33
34 48 humid conditions (Bordy et al., 2005) returned. This change in climate state is evidenced by the
35
36
37 49 preservation of a highly diverse megaf flora in the Molteno Formation (Anderson and Anderson,
38
39 50 1985; Bamford, 2004). The interpretation of such patterns is dependent not only on the
40
41
42 51 taphonomy and nature of the mega- and microfloral assemblages (e.g., Gastaldo et al., 2005,
43
44 52 2021), but also on their frequency of occurrence and sampling intensity over the stratigraphic
45
46
47 53 interval of interest (DiMichele and Gastaldo, 2008). Ultimately, though, the interpretations of
48
49 54 such patterns are controlled by the rock record, itself.
50

51
52 55 Rocks of the main Karoo Basin are exposed across nearly two-thirds of South Africa and
53
54 56 are assigned to the Karoo Supergroup (Fig. 1). They represent deglacial sediments of the latest
55
56
57 57 Carboniferous and early-to-middle Permian that transition to fully continental pedogenically
58
59

1
2
3
4 58 modified floodplain (paleosols of various type), fluvial, and lacustrine deposits that persisted into
5
6
7 59 the Triassic. Fully terrestrial deposition begins in the Middle Permian (Guadalupian; Rubidge et
8
9 60 al., 2012) and continues into the Lower Jurassic (Bordy et al., 2020) before the emplacement of
10
11
12 61 the extensive Karoo-Ferrar Dolerites across southern Africa and Antarctica (Pleinsbachian;
13
14 62 Svensen et al., 2012). The strata reported to straddle the Permian–Triassic boundary (PTB) have
15
16
17 63 been interpreted to represent a “continuous” record of sedimentation in localities of the Eastern
18
19 64 Cape and Free State provinces (e.g., Smith, 1995; Ward et al., 2005; Smith and Botha-Brink,
20
21
22 65 2014; Botha et al., 2020; Viglietti et al., 2021). Advances in discriminating a sequence-
23
24 66 stratigraphic model (e.g., Gastaldo and Demko, 2011) in this part of the basin, coupled with
25
26
27 67 geochronometric and paleomagnetic data in stratigraphic frameworks for classic PTB localities,
28
29 68 now constrain this part of the paleontological record and provide a more comprehensive
30
31
32 69 understanding of it (Gastaldo et al., 2015, 2018, 2020a, 2021). We will explore these advances
33
34 70 that allow us to assess: the distribution, through space and time, of paleobotanical assemblages,
35
36
37 71 therein; and the vegetational response in the Karoo Basin, testing the rapidity of turnover in this
38
39 72 part of Gondwana. We will present lessons learned that should be applied in other, fully
40
41
42 73 continental settings regardless of age.

44 74 **2. Considerations of Upper Permian and Lower Triassic Geology**

45
46
47 75 The sedimentary succession known as the Karoo Supergroup is subdivided into the
48
49 76 Dwyka (Carboniferous–Lower Permian), Ecca (Lower–Middle Permian), Beaufort (Middle
50
51
52 77 Permian–Middle Triassic), Stormberg (Upper Triassic–Lower Jurassic), and Drakensberg (Lower
53
54 78 Jurassic) Groups. The Beaufort Group (Fig. 2) is exposed in the main Karoo Basin (Fig. 1;
55
56
57 79 Johnson et al., 2006) and the Lebombo Basin in the eastern part of South Africa (Bordy and
58
59

1
2
3
4 80 Prevec, 2008, 2015). It consists primarily of a sandstone-and-mudstone succession, that is
5
6
7 81 monotonous in physical characteristics, and attains a thickness of >2500 m in the southern part of
8
9 82 the basin (Viglietti et al., 2017). The absence of a distinct set of physical criteria to distinguish
10
11
12 83 lithostratigraphic units led early workers to rely on an abundant and diverse fossil-vertebrate
13
14 84 fauna. These faunas are dominated by pre-mammalian terrestrial tetrapods and have been used as
15
16
17 85 the basis for its subdivision (Smith et al., 2020) into what are accepted as Permian and Triassic-
18
19 86 aged rocks. Geochronometric (Fig. 2; Rubidge et al., 2013; Day et al., 2015; Gastaldo et al.,
20
21
22 87 2015, 2021) and paleomagnetic (Gastaldo et al. 2018, 2020a, 2021) constraints in
23
24 88 lithostratigraphic context now allow for traditional litho- and biostratigraphic paradigms to be
25
26
27 89 evaluated and better correlated with global standards. What once was promoted as a simple
28
29 90 solution to distinguish stratigraphic units, the use of vertebrate biostratigraphy, is now
30
31
32 91 demonstrated to be complicated and problematic (see discussion in Gastaldo et al., 2021).

33
34 92 The latest Permian and earliest Triassic deposits occur in the Balfour and Katberg
35
36
37 93 formations where several formal and informal lithostratigraphic members are recognized (Fig. 2).
38
39 94 Changhsingian-aged deposits likely begin in the Daggaboersnek or Barberskrans (informal
40
41
42 95 Ripplemead Member; Viglietti et al., 2017) member and extend through the Elandsberg and
43
44 96 Palingkloof members into the basal Katberg Formation (Gastaldo et al., 2020a, 2021). Currently,
45
46
47 97 the remainder of the Katberg Formation is assigned to the Lower Triassic. The end-Permian
48
49 98 terrestrial event in Australia (e.g., Fielding et al., 2019), as identified by palynostratigraphy and
50
51
52 99 constrained by geochronology, is first identified in the Katberg Formation (Gastaldo et al., 2019).
53
54 100 Here, vegetational changeover (*Dulhuntyispora parvithola* to *Playfordiaspora crenulata*
55
56
57 101 palynozones; Mays et al. 2020) dates younger than 252.24 ± 0.11 Ma (Gastaldo et al., 2020a) in a
58
59
60
61
62
63
64
65

1
2
3
4 102 fluvial-siltstone trough fill positioned above the vertebrate-defined PTB as reported on farm
5
6
7 103 Nooitgedacht (Botha et al., 2020).

8
9 104 The initial vertebrate-defined extinction-and-assemblage turnover model (Ward et al.,
10
11
12 105 2000, 2005) was reported to have occurred over a stratigraphic thickness of ~60 m in the
13
14 106 Palingkloof Member, temporally constrained to represent between 10 ka and 100 ka (Smith and
15
16
17 107 Botha-Brink, 2014). With the addition of the high-resolution age date in the Palingkloof Member
18
19 108 (Gastaldo et al., 2020a), Viglietti et al. (2021) revised the vertebrate model and now interpret a
20
21
22 109 protracted faunal assemblage change occurred over a stratigraphic interval of 100 m with a
23
24 110 protracted mass-extinction event lasting 1 Ma. In this model, the pre-extinction Upper
25
26
27 111 *Daptocephalus* Assemblage Zone (AZ; *L. maccaigi*–*Moschorhinus* subzone) is replaced by new
28
29 112 taxa reported to have their first appearance datums (FAD) in the post-extinction *Lystrosaurus*
30
31
32 113 *declivis* AZ. Recently, Gastaldo et al. (2021) demonstrated that the diagnostic taxa used to
33
34 114 circumscribe each of the Upper *Daptocephalus* and *L. declivis* assemblage zones are preserved in
35
36
37 115 coeval strata in the Eastern Cape Province. These purportedly pre-extinction and post-extinction
38
39 116 diagnostic taxa are in Changhsingian deposits yielding microfloral assemblages that are of the
40
41
42 117 Late Permian, *Glossopeteris*-dominated, *D. parvithola* palynozone (Fig. 2).

43
44 118 The lithostratigraphic position of the PTB in the Karoo, if present, likely is somewhere in
45
46
47 119 the lower Katberg Formation (Gastaldo et al., 2021). Currently, though, it is unconstrained by
48
49 120 either geochronologic or magnetostratigraphic data. Viglietti et al. (2017) reaffirm the disparity
50
51
52 121 in available stratigraphic sections between southern localities in the Eastern Cape Province (e.g.,
53
54 122 Lootsberg Pass), close to the provenance of sediment supply, and those in distal parts of the basin
55
56
57 123 in the Free State Province (e.g., Bethulie; Fig. 1). Criteria to identify the Katberg Formation
58
59
60
61
62
63
64
65

1
2
3
4 throughout the basin relied heavily on the presence of intraformational conglomerate lag in thick
5
6 fluvial sandstone (e.g., Smith, 1995; Retallack et al., 2003). The presence of pedogenic nodule
7
8 conglomerate (PNC) was considered as a unique and diagnostic feature of Triassic rivers
9
10 assigned to the Katberg Formation, believed to have formed in the wake of the aridity interpreted
11
12 to have been associated with the end-Permian event and loss of vegetation (Ward et al., 2000,
13
14 2005; Smith and Botha-Brink, 2014). Other workers have demonstrated that these
15
16 intraformational lag deposits are a common feature of the Beaufort Group. They occur in the
17
18 Middle Permian Abrahamskraal Formation (Katsiaficas et al., 2010) and extend throughout the
19
20 upper Permian Balfour Formation (Fig. 2; e.g., Viglietti et al., 2017; Gastaldo et al., 2017, 2019,
21
22 2021). Such intraformational lag deposits are the result of landscape degradation (Gastaldo and
23
24 Demko, 2011), concentrating resistant and refractory calcite-cemented soil nodules at the base of
25
26 newly established rivers and their adjacent floodplains. In contrast to their concentration as river
27
28 sediment, soil remnants—the fine siliciclastics (very fine sand, silt, and clay)—were eroded and
29
30 transported basinward, removing any evidence of their existence except for when tuffaceous
31
32 deposits can be dated geochronometrically (Gastaldo et al., 2018, 2021). The presence of PNC
33
34 lags in rivers, then, represent “ghost” landscapes (Gastaldo et al., 2020b); they are the only
35
36 evidence of conditions that prevailed where no stratigraphic record now exists. Landscape
37
38 erosion (fluvial and interfluvial paleosols) resets sediment accumulation in a new depocenter,
39
40 and changes the potential for preservation of floral elements (Gastaldo and Demko, 2011). This
41
42 episodic, but ongoing, set of processes on land results in a stratigraphic record replete with highly
43
44 condensed sections of variable thickness and temporal resolution in different parts of the basin.
45
46 Hence, it is highly unlikely that a lithostratigraphic interval in which the PTB will occur
47
48
49
50
51
52
53
54
55
56
57
58
59
60
61
62
63
64
65

1
2
3
4 146 exclusively in the Katberg Formation.
5

6 7 147 **3. Paleobotany over the Permian–Triassic Transition** 8

9 148 Our knowledge of the reported megafossil and microfossil assemblages in the Balfour
10
11 and Katberg formations, to date, are restricted to a few localities. In Kwazulu-Natal Province
12 149
13 these include: farms Christina and Moorfield (Classen, 2008) and Clouston farm (Prevec et al.,
14 150
15 2009), previously assigned to the Normandien Formation that is now combined with the Balfour
16 151
17 Formation (Groenewald et al., 2022); several isolated megafloreal localities that are unconstrained
18 152
19 in that formation (Mooi River [Lacey et al., 1975]; Wagendrift, [Zavada and Mentis, 1992;
20 153
21 Selover and Gastaldo, 2003]; Bulwer [Lacey, 1976; Gastaldo et al., 2005]; and Loskop [Gastaldo
22 154
23 et al., 2005; McLoughlin et al., 2021]); and a number of localities from which permineralized
24 155
25 wood is reported (Bamford, 1999, 2004). In the Eastern Cape Province (Fig. 3A), paleobotanical
26 156
27 assemblages are known from: Wapadsberg Pass (Prevec et al., 2010; Gastaldo et al., 2014), farms
28 157
29 Blaauwater and Tweefontein (Gastaldo et al., 2017, 2021), Old Lootsberg Pass (Gastaldo et al.,
30 158
31 2018), and Carlton Heights (Retallack et al., 2003; Gastaldo et al., 2005). And, localities in the
32 159
33 Free State Province (Fig. 3B) include: farms Donald 207 (=Fairydale; Smith and Botha-Brink,
34 160
35 2014; Barbolini et al., 2018), Bethel (Gastaldo et al., 2005, 2019) and Tussen die Riviere, and
36 161
37 Nooitgedacht (Botha et al., 2020; Gastaldo et al., 2020a). A general overview of the character
38 162
39 and diversity of megafloreal and microfloral assemblages follow.
40 163
41
42
43
44
45
46
47
48

49 164 **3.1 Megafloora** 50

51 165 **3.1.1 Adpression floras** 52 53

54 166 The predominant preservational mode of megafloreal assemblages is adpression where, in
55
56 some instances, cuticular remains can be retrieved from littered bedding surfaces. In many cases,
57 167
58
59
60
61
62
63
64
65

1
2
3
4 168 though, organic remains have decayed or been lost, leaving faint-to-well defined morphological
5
6
7 169 features impressed into the sediment in which these were buried. Robust axes, such as
8
9
10 170 equisetalean *Paracalamites*, as well as lycopsid and unidentifiable axes, are preserved in fine- to
11
12 171 very fine-grained sand and finer clastic sediments. In contrast, leaves and other aerial parts are
13
14 172 almost exclusively restricted to coarse-to-fine siltstone; claystone is uncommon in this part of the
15
16
17 173 succession and, where encountered, may preserve cyclical beds of leaf litter (e.g., Bulwer;
18
19 174 Gastaldo et al., 2005). Leaves in fine-grained sandstone and siltstone can be identified by their
20
21
22 175 persistent venation without intervening lamina, most often as impressions. Rarely have *in situ*
23
24 176 roots and/or rooting systems been encountered (e.g., *Vertebraria*; Gastaldo et al., 2014) despite
25
26
27 177 the fact that paleosols dominate the sedimentological record in the basin.
28

29 178 Wetland taxa prevail in collections and include equisetaleans, rare lycopsids and ferns,
30
31
32 179 and gymnosperms, whereas the most common elements are assigned to Glossopteridales (Fig.
33
34 180 4A, B). Aerial parts of horsetails include axes and lateral branches with whorled leaves, and
35
36
37 181 reproductive cones. These are assigned to two orders and three families: Schizoneuraceae (e.g.,
38
39 182 *Schizoneura*) and Phyllotheceae (e.g., *Paracalamites*, *Phyllothea*) in the Equisetales, and
40
41
42 183 Sphenophyllaceae (e.g., *Trizygia*) in the Sphenophyllales (Fig. 4C). Very few examples of
43
44 184 lycopsids have been recovered, and assignment of defoliated specimens to the club mosses can
45
46
47 185 be complicated by their preservational state (e.g., Prevec et al., 2009). This is not the case for
48
49 186 ferns. This is despite their generally small specimen size and generalized morphologies, resulting
50
51
52 187 in their assignment to the form taxon *Sphenopteris*. In contrast, *Glossopteris* leaf morphologies
53
54 188 are relatively diverse and vary in both size and venation patterns. Early reports assigned
55
56
57 189 specimens to established species (Lacey, 1976) but with recognition that leaf characteristics vary
58
59
60
61
62
63
64
65

1
2
3
4
5 190 in sample populations, a morphotype approach is applied to their systematization (e.g., Claassen,
6
7 191 2008; Prevec et al., 2009, 2010; Botha et al., 2020). At least 30 different morphotypes of
8
9 192 *Glossopteris* are recognized, to date, in these latest Permian assemblages. These morphotypes are
10
11
12 193 in addition to leaves formally assigned to *Glossopteris conspicua* and *G. elongata* (Lacey 1976),
13
14 194 *G. symmetrifolia* (Gastaldo et al., 2017), and *G. angustifolia* and *G. linearis* (Botha et al., 2020).
15
16
17 195 Often it is possible to find evidence of plant-insect interaction in glossopterids (Fig. 5; Prevec et
18
19 196 al., 2009, 2010; McLoughlin et al., 2021).
20

21
22 197 There is a dearth of paleobotanical material, to date, in rocks assigned to the Lower
23
24 198 Triassic. Isolated and dispersed fossils in the Katberg Formation are preserved on bedding in
25
26
27 199 fluvial fine-grained sandstone and sandy siltstone and, generally, unidentifiable (e.g., Gastaldo et
28
29 200 al., 2005). Retallack et al. (2003, p. 1147), though, report the presence of what were, then,
30
31
32 201 considered to be exclusively Triassic taxa from Bethulie and Carlton Heights. These were
33
34 202 described as “plant hash” but not illustrated. The samples were transferred to the authors
35
36
37 203 subsequent to the paper’s publication, and now are curated in the paleobotanical collections of
38
39 204 the Evolutionary Studies Institute. The small collection includes the original specimen number as
40
41
42 205 assigned by Retallack and a letter of transmittal (samples curated in the paleobotanical collection,
43
44 206 University of Witwatersrand, Johannesburg). Taxa identified to genus include: *Lepidopteris* (Fig.
45
46
47 207 6A, B), *Pagiophyllum* (Fig. 6C, D), *Cladophlebis* (Fig. 6E), and *Samaropsis* (Fig. 6F).
48

49 208 **3.1.2 Permineralized wood**

50

51
52 209 Less common in latest Permian and Lower Triassic rocks are permineralized woods (Fig.
53
54 210 7), which may be reflected in the reported diversity of taxa. Bamford (1999, 2000, 2004)
55
56
57 211 identified a single genus in this interval in which two species are recognized: *Agathoxylon*
58
59

1
2
3
4 212 *africanum* and *A. karooensis*. *Agathoxylon africanum* (Fig. 7E) is a long ranging taxon that
5
6
7 213 appears in the Lopingian and continues into the Middle Triassic of southern Africa (Bamford and
8
9 214 Philippe, 2001). In contrast, *A. karooensis* (Fig. 7F) is only known from uppermost Permian
10
11
12 215 strata. Recently, Bamford et al. (2020) recognized wood assignable to *Australoxylon natalense*
13
14 216 and *A. teixeirae* (Fig. 7D) in the latest Permian Middleton Formation of the Eastern Cape
15
16
17 217 Province. This wood type is very similar to that of *Vertebraria*, the woody roots of
18
19 218 glossopteridalean trees.
20

21 219 **3.2 Microfloras**

22
23
24 220 There are rare occurrences of palynological assemblages documented from surficial
25
26
27 221 outcrops in the upper Permian–lower Triassic succession (e.g., Prevec et al., 2009, 2010;
28
29 222 Barbolini et al., 2016, 2018; Gastaldo et al., 2015, 2017, 2019, 2020a, 2021). There are a few
30
31
32 223 studies conducted on drill core in the main Karoo and southern Africa, focused primarily in the
33
34 224 coal-bearing Ecca Group (e.g., MacRae, 1988; Falcon, 1989; Aitken, 1994; Wagner et al., 2019)
35
36
37 225 where results are available in unpublished theses and dissertations (e.g., Mahabeer, 2017). Other
38
39 226 studies (Ruckwied et al., 2014; Götz et al., 2017) have misinterpreted the stratigraphy and
40
41
42 227 palaeoenvironments (see comments by Cole, 2017; Cole and Barbolini, 2019) and have not taken
43
44 228 this field further. Basin-wide sampling from the vertebrate biozones, together with radiometric
45
46
47 229 dating, has produced a broad overview and pollen biostratigraphy (Barbolini et al., 2016, 2018),
48
49 230 but a high resolution, core-sourced profile is still lacking for the South African Karoo Basin. The
50
51
52 231 quality of dispersed assemblages is dependent on the depth of weathering of surficial exposure
53
54 232 and, more importantly, the thermal history of the rocks in which they are preserved. Palynomorph
55
56
57 233 color ranges from orange-yellow (e.g., Fig. 8C), indicative of a thermal maturation index (TMI)
58
59
60
61
62
63
64
65

1
2
3
4 234 ~2, to brownish black and black (Fig. 8D, F), indicative of a TMI approaching or >4 (Marshall,
5
6 235 1990). Hence, post-depositional preservation potential is dependent, primarily, on the
7
8
9 236 emplacement of Jurassic-aged dolerite dykes associated with the Karoo-Ferrar Large Igneous
10
11
12 237 Province. Thermal maturation of the host rock where temperatures exceeded 200° C has resulted
13
14 238 in the “cooking” of organics and, in many instances, the loss of diagnostic features that would
15
16
17 239 allow for systematic identification of any residual palynomorphs.
18

19 240 Dolerite intrusions are ubiquitous throughout the basin Main Karoo basin but are rare in
20
21
22 241 the Ellirus Basin, Waterberg Coalfield, a small basin in northern South Africa. Here, Wagner et
23
24 242 al. (2019) have been able to correlate the maceral types with palynology and environmental
25
26
27 243 interpretations. They processed bulk samples from coal seams in the Vryheid Formation and
28
29 244 overlying Grootegeeluk Formation and found that these assemblages correlated with the previous
30
31
32 245 work of Falcon (1986, 1989). Inertinite was found to be dominant together with tree-fern spores
33
34 246 and a diversity of other palynomorphs, indicating a wetland setting and cooler climate. In
35
36
37 247 contrast, the overlying Grootegeeluk Formation has high vitrinite/vitrite and is dominated by
38
39 248 bisaccates, indicating a wet gymnosperm forest under a warmer and more seasonal climate that
40
41
42 249 promoted rapid growth (Wagner et al., 2019).
43

44 250 Most productive assemblages are dominated by taeniate pollen assigned to the
45
46
47 251 Glossopertidales (Fig. 8E–G) and spores of groundcover sphenophyllaleans (Fig. 8B–C) and
48
49 252 ferns (Fig. 8D). Such taxa originate from vegetation that grew in wetlands and landscapes that
50
51
52 253 experienced seasonally wet conditions. In several rare instances, though, late Permian
53
54 254 assemblages contain a low to moderate proportion of other gymnosperm groups, macroscopic
55
56
57 255 remains of which are not found in these rocks (Prevec et al., 2010; Gastaldo et al., 2015, 2017).
58
59
60
61
62
63
64
65

1
2
3
4 256 These taxa include pollen with Voltzian conifer, Peltasperm, and Corystosperm affinities (Fig.
5
6
7 257 8I–K), and are preserved in sediments associated with seasonally dry paleosol intervals where
8
9 258 calculated Mean Annual Temperatures averaged $\sim 8.7 \pm 4.4^\circ \text{C}$ and Mean Annual Precipitation
10
11
12 259 was $890 \pm 181 \text{ mm/yr}$ (Gastaldo et al., 2020b). Many of these taxa were once considered
13
14 260 indicative of Triassic vegetation by other workers (e.g., Eshet et al., 1995) but, now, are known
15
16
17 261 to have their first appearance datums in the Permian (e.g., Blumenkemper et al., 2019).

18 19 262 **4. Spatial and Temporal Distribution of Karoo Plant Assemblages**

20
21
22 263 The majority of the Karoo bedrock is covered either in dwarf succulent shrubby
23
24 264 vegetation, talus comprised of resistant sandstone and/or dolerite boulders, or both which may be
25
26
27 265 up to depths of several meters. Upper Paleozoic and Lower Mesozoic Karoo strata typically are
28
29 266 exposed either as thin surface outcrops in quarries of a few meters in relief, or in narrow
30
31
32 267 erosional drainage gullies (dongas). Dongas vertically traverse escarpments, which are capped by
33
34 268 resistant lithologies. In some instances it is possible to measure a stratigraphic section that
35
36
37 269 approaches 300 m, although gradients at higher elevations often are difficult to access limiting
38
39 270 observations to resistant sandstones. In general, though, donga exposures are limited in width to
40
41
42 271 less than a few meters, depending on their elevation on the mountainside. Hence, the availability
43
44 272 of exposures where fossiliferous plant beds can encountered or traced laterally, described in
45
46
47 273 context, and sampled is limited to lower elevations. In contrast, vertebrate remains have been
48
49 274 collected from surface exposures where incompetent matrix has weathered around calcified
50
51
52 275 skeletons and skeletal elements.

53 54 276 **4.1 Historical and Geographic Context of Plant Sites**

55
56
57 277 Vertebrate paleontology has been the driving force in South Africa for more than a
58
59

1
2
3
4 278 century, and many of the Upper Permian–Lower Triassic fossil-plant localities are tied directly to
5
6
7 279 collection sites where megafaunal elements are reported. In essence, though, there are two, basic
8
9 280 geographic areas from which the Permian–Triassic vertebrate database originates. The first is in
10
11
12 281 the Eastern Cape Province where they are described as “classic” PTB sections. Here, localities
13
14 282 (variously named in the literature for same site; Fig. 3) include: Old Wapadsberg Pass
15
16
17 283 (-31.921867°, 24.897100°), Lootsberg Pass (-31.848384°, 24.077036°), Tweefontein of Ward et
18
19 284 al. (2005; -31.838050°, 24.847217°); Tweefontein of Gastaldo et al. (2018, 2021; -31.824033°,
20
21
22 285 24.812067°; to clarify confusion about vertebrate-collection sites, see Gastaldo et al, 2017,
23
24 286 2021); Old Lootsberg Pass (-31.795743°, 24.812067°); Carlton Heights (-31.29228°, 24.95152°),
25
26
27 287 and KommandoDrif Dam (-32.138540°, 26.083277°). The geographic straight-line distance
28
29 288 between Lootsberg Pass and: Old Lootsberg Pass is 9.5 km to the NW, Wapadsberg Pass is 9.5
30
31
32 289 km to the SE, Carlton Heights is 45 km to the NW, and Kommandodrif Dam is 115 km to the
33
34 290 ESE. The second generalized area is in the Free State Province, where the distance from
35
36
37 291 Lootsberg Pass is >200 km to the NE. Here, reported PTB localities include: Bethel
38
39 292 (-30.422040°, 26.270160°) and Heldenmoed (-30.417117°, 26.264167°) farms, Donald 207
40
41
42 293 (=Fairydale of Smith and Botha-Brink, 2014; -30.407000°, 26.237710°), and Nooitgedacht (-
43
44 294 30.32530°, 25.93132°). Retallack et al. (2003, their fig. 3B) report a laminated succession at
45
46
47 295 Bethel farm, located in Tussen Die Riviere game park (Fig. 3B), that is fault bounded and cannot
48
49 296 be correlated with rocks on other localities (Gastaldo et al., 2009). Greater than 80% of the
50
51
52 297 vertebrate specimens used in the development of the reported vertebrate-defined extinction event,
53
54 298 equated to the PTB extinction (Ward et al., 2005; Smith and Botha-Brink, 2014; Viglietti et al.,
55
56
57 299 2021), were recovered from ~10 km² area on farms Bethel, Heldenmoed, and Donald 207, and
58
59
60
61
62
63
64
65

1
2
3
4 300 Tussen Die Riviere nature reserve (Gastaldo et al., 2019). Hence, these “classic” Eastern Cape
5
6
7 301 and Free State localities have been the primary focus of our efforts over the past 20 years.
8

9 302 **4.2 Stratigraphic Context of Plant Sites**

10
11
12 303 The total stratigraphic thickness of measured sections that form the basis of the current
13
14 304 contribution is >3750 m, encompassing the above localities in which each is reported to contain
15
16
17 305 the vertebrate-defined PTB. Where outcrop is limited or inaccessible, such as the Carlton
18
19 306 Heights, Kommandodrif Dam, or Nooitgedacht localities, a single measured section was acquired
20
21
22 307 beginning at the base of the koppie. In other localities where several dongas traverse the
23
24 308 mountainside, as many as ten or more measured sections of various stratigraphic length were
25
26
27 309 correlated across the escarpment using laterally extensive sandstone bodies (e.g., Gastaldo et al.,
28
29
30 310 2021). Table 1 presents the number of measured sections (including unpublished observations),
31
32 311 their total stratigraphic thickness, the number and type of plant-bearing intervals for each locality,
33
34 312 and pertinent citations.

35 36 37 313 4.2.1 Eastern Cape Province

38
39 314 The easternmost set of classic localities centers in-and-around Wapadsberg Pass. Here,
40
41
42 315 sections are published for Old and New Wapadsberg Pass, and for donga exposures on farm
43
44 316 Quaggasfontein; two measured sections have been described on farm Pienaarsbaaken
45
46
47 317 (unpublished). A total of 1,130 m of section are detailed from these 12 successions.
48
49 318 Glossopterid-dominated assemblages are preserved as bedded litters in the basal intervals of the
50
51
52 319 Old and New Wapadsberg sections (Prevec et al., 2010), whereas isolated aerial debris is rare
53
54 320 higher in the section. Here, only nine horizons account for our understanding of the adpression
55
56
57 321 assemblages, and permineralized wood fragments have been encountered scattered over only two
58
59
60
61
62
63
64
65

1
2
3
4 322 surfaces. In contrast, we have recovered ten spore-and-pollen assemblages and palynomorphs
5
6
7 323 display a range of preservational qualities and thermal indices of alteration (Fig. 8). Palynological
8
9 324 assemblages are associated with bedded litters in the basal intervals, whereas other horizons
10
11
12 325 preserve them in fine-grained laminated siltstone higher in these sections. In contrast to
13
14 326 megafloral assemblages, glossopterid pollen grains are often admixed with those of other
15
16
17 327 gymnosperm groups for which there is no evidence in the megafloral record (Gastaldo et al.,
18
19 328 2018). To date, though, we have not encountered or recovered either adpression or palynological
20
21
22 329 assemblages higher than the Balfour or Katberg formations in-and-around Wapadsberg Pass.
23

24 330 The area including, and west of, Lootsberg Pass is the second classic region in which the
25
26
27 331 vertebrate-defined extinction is reported and paleobotanical assemblages described. Exposures
28
29 332 along farm roads and in dongas spread across the escarpment can be traced over a distance of ~10
30
31
32 333 km. These are found on the Kingwill farms, which include Tweefontein (*sensu latu*) and
33
34 334 Blaauwater. Over this expansive area we have reported >1650 m in 23 measured sections; there
35
36
37 335 are several, shorter measured-and-described intervals that remain unpublished. Similar to
38
39 336 Wapadsberg Pass sites, glossopterids dominate the megaf flora and microflora in seven and two
40
41
42 337 localities, respectively (Table 1). All fossils are preserved in olive-gray siltstone.
43

44 338 Megafloral preservation in olive-gray siltstone is also the case at Kommandodrif Dam
45
46
47 339 (N=2) and Carlton Heights (N=2) where isolated aerial debris is reported (Gastaldo et al., 2005).
48
49 340 A single horizon of isolated debris occurs in the Palingkloof Member at Carlton Heights in a
50
51
52 341 bedded interval that was reported to represent the PTB (Retallack et al., 2003). The assignment
53
54 342 of that succession to the end-Permian marine equivalent was based on the assumption, at the
55
56
57 343 time, that a unique “laminite” facies occurred at a single, basin-wide horizon and marked the
58
59
60
61
62
63
64
65

1
2
3
4 344 event. This assumption of a single, heterolithic, contemporaneous interval with a basin-wide
5
6
7 345 correlation has been shown to be in error at the Bethel farm locality (Gastaldo et al., 2009) where
8
9 346 it was first introduced into the literature (Smith, 1995). The most recent data demonstrate that the
10
11
12 347 “laminite” interval believed to mark the PTB as reported by previous authors at Lootsberg Pass
13
14 348 (Ward et al., 2000, 2005; Retallack et al., 2003), for example, lies stratigraphically below an
15
16
17 349 early Changhsingian U-Pb CA-ID-TIMS age of 252.43 ± 0.19 Ma (Gastaldo et al., 2021). And,
18
19 350 similar to Wapadsberg Pass, we have not encountered assemblages higher in the Katberg
20
21
22 351 Formation except at Carlton Heights.

23
24 352 Isolated aerial plant debris is rarely encountered in the Katberg Formation, where we have
25
26
27 353 measured 380 m of stratigraphy in eight sections. Here, plant hash is scattered atop bedding in
28
29
30 354 very fine sandstone and we have found identifiable debris on only a single horizon (Gastaldo et
31
32 355 al., 2005). Additional, scattered megafloral elements (Retallack et al., 2003; Fig. 6) and 22
33
34 356 horizons have been reported to yield microfloral assemblages, spread over an interval of 59 m
35
36
37 357 (Steiner et al., 2003). The succession from which these palynological assemblages were
38
39 358 recovered by Steiner et al. (2003) appears not to have been sampled at the classic exposure along
40
41
42 359 the M9. Rather, sampling was done on exposures somewhere along the M10 (N. Tabor, pers.
43
44 360 comm. 2019) for which no GPS coordinates are published. We have been unable to replicate the
45
46
47 361 observations of Steiner et al. (2003) in the Carlton Heights succession (Pace et al., 2009).

48 49 362 4.2.2 Free State Province 50

51
52 363 The vertebrate database on which the end-Permian vertebrate extinction is interpreted
53
54 364 (Ward et al., 2005; Smith and Botha-Brink, 2014; Viglietti et al., 2021) originates from three
55
56
57 365 adjacent farms in the Free State Province: Bethel, Heldenmoed, and Donald 207/Fairydate (Fig.
58
59
60
61
62
63
64
65

1
2
3
4 366 3B; Gastaldo et al., 2019). We have reported a total of 1130 m of stratigraphy encompassing 22
5
6
7 367 measured sections of various lengths across the area in addition to several, unpublished short
8
9 368 stratigraphic sections (Table 1). Although isolated resistant equisetalean or unidentifiable axes
10
11
12 369 may be encountered infrequently, identifiable megafloral remains are very rare. To date, only two
13
14 370 fossiliferous intervals have been found on the Bethel and Heldenmoed farms; no bedded litter has
15
16
17 371 been encountered on farm Donald 207. There is a similar dearth of recoverable palynological
18
19 372 assemblages, with a single productive interval reported from Donald 207 farm, high in the
20
21
22 373 section, that is assigned to the *Protohaploxypinus microcorpus* palynozone (Table 1; Fig. 2).
23
24 374 Rocks on farm Nooitgedacht have been more productive.

25
26
27 375 Nooitgedacht outcrops occur around two koppies on the farm: Loskop and Spitskop.
28
29 376 Botha et al. (2020) illustrate one composite section, totaling 86 m of stratigraphy, from each hill.
30
31
32 377 We have documented a single, 90-meter section from Loskop (Gastaldo et al., 2020a;
33
34 378 unpublished field notes 08/2022). Botha et al. (2020) report five intervals in which megafloral
35
36
37 379 remains are preserved, and figure specimens assigned to *Paracalamites*, *Glossopteris* and its
38
39 380 reproductive propagules, and an indeterminate fern genus. Gastaldo et al. (2020a) report two
40
41
42 381 horizons in which palynomorphs are well preserved. The lower interval occurs directly above a
43
44 382 zircon-age date of 252.24 ± 0.11 Ma from a pristine ash-fall deposit, assigned to the
45
46
47 383 *Dulhuntyispora parvithola* palynozone. The upper assemblage is preserved ~10 m higher, above
48
49 384 an erosional surface at the base of a down-cutting fluvial regime, that is assigned to the
50
51
52 385 *Playfordiaspora crenulata* zone (Fig. 2).

53 54 386 4.2.3 Lesson 1: Proportional representation of paleobotanical assemblages 55

56
57 387 In total, 29 horizons macrofossil assemblages, excluding beds on which isolated axes or
58
59
60
61
62
63
64
65

1
2
3
4 388 mesofossil organic drapes occur, and four beds from which permineralized woods have been
5
6
7 389 encountered and described spanning the uppermost Permian and lower Triassic succession. In
8
9 390 contrast, at least 48 beds (Table 1) have been reported to yield productive palynological
10
11
12 391 assemblages over the same interval. Considering that these data originate from >3750 m of total
13
14 392 measured section, megafloral remains are preserved in < 1% of the available rock record (0.9%
15
16
17 393 all megafloral elements; permineralized wood = 0.1%, adpressions = 0.8 %). Although spore-
18
19 394 and-pollen assemblages are encountered more frequently in the literature (1.3%; Table 2), they
20
21
22 395 are preserved in only 0.4% of our measured sections. These very low values in the Karoo are
23
24 396 consistent with data from other fully continental, Upper Permian–Lower Triassic successions
25
26
27 397 documented in the Bogda Mountains, Xinjiang Province, western China (Gastaldo et al., in
28
29 398 press). There, permineralized wood is encountered in <2% and adpression assemblages in <1%
30
31
32 399 of depositional high-order cycles, which vary in stratigraphic thickness across nine localities
33
34 400 extending over 100 km distance. In fact, if each western China assemblage was preserved
35
36
37 401 throughout the entirety of 1 m of measured section, these intervals would represent a mere 0.55%
38
39 402 of the entire Bogda Mountain measured stratigraphic record of 4,709 m (Gastaldo et al., in press).
40
41
42 403 In reality, identifiable macrofloral remains generally are limited to intervals of centimeters to
43
44 404 decimeters reducing their proportionality in the rock record.

405 **4.3 Time and stratigraphic relationships**

46
47

48
49 406 The continental stratigraphic record is notoriously incomplete and the temporal
50
51
52 407 relationships between units are difficult to interpret, in large part, because of a scarcity of datable
53
54 408 sediments. Considerable time is “locked” in paleosols as diastems, with most fluvial sediments in
55
56
57 409 adjacent deposits representing various stages of riverine processes prior to either avulsion,
58
59
60
61
62
63
64
65

1
2
3
4
5 410 abandonment, or a resetting of the land surface in response to landscape degradation or a
6
7 411 basinward shift in depocenters. Continued erosion and reworking of unconsolidated sediments on
8
9 412 land are the norm, and not the exception, and these processes are influenced by a combination of
10
11
12 413 climatic or tectonic factors, or both (Bull, 1991; Gastaldo and Demko, 2011). Erosional bounding
13
14 414 surfaces, often incised into underlying deposits and found at the base of fluvial sandstone bodies,
15
16
17 415 are evidence of an interval of landscape erosion and degradation. These surfaces mark a hiatus in
18
19 416 time and, hence, a gap of some duration in the stratigraphic record longer than paleosol diastems.
20
21
22 417 Nevertheless, terrestrial successions in the Karoo, and elsewhere, often are reported to represent
23
24 418 “continuous” sedimentation. Such broad assumptions have allowed workers, in turn, to interpret
25
26
27 419 biological patterns from the paleontological assemblages preserved, therein, over the interval of
28
29 420 interest no matter how infrequent these may be in the stratigraphic record (Gastaldo et al., in
30
31
32 421 press). Yet, without any geochronologic or rock magnetic data with which to place temporal
33
34 422 boundaries onto the stratigraphic record, such ecological interpretations only can be considered
35
36
37 423 as broad working hypotheses subject to revision. The stratigraphy and fossil record of the Karoo
38
39 424 is no exception and can serve as a model for understanding other continental successions.

40 41 42 425 **4.3.1 Geochronology**

43
44 426 The gold standard for establishing a maximum age constraint on a deposit is a U-Pb CA-
45
46
47 427 ID-TIMS age estimate obtained from individual zircon grains, of a euhedral, pristine nature,
48
49 428 recovered from a volcanogenic sediment. Values of uranium-and-lead isotopes from individual
50
51
52 429 crystals in a sample suite are plotted on a Concordia diagram, which is a graphical way to
53
54 430 evaluate the internal consistency of U-Pb data. Concordant isotopic compositional space is
55
56
57 431 marked by the concordia line, a curve, and isotopic ratio measurements are figured as confidence
58
59
60
61
62
63
64
65

1
2
3
4 32 ellipses (see: Gastaldo et al., 2015, 2021). Concordant samples that plot near to, or overlap with,
5
6
7 33 the concordia line represent geochronological reliability (Ludwig, 1998). Volcanogenic airfall
8
9 34 deposits are exceedingly rare and easily eroded on land. A rule-of-thumb to identify these in the
10
11
12 35 field is the “what doesn’t belong here” approach, which is based on their unusual color (light
13
14 36 gray [Munsell color N7] to white [N8], in general), texture (silicification, a lithology appearing
15
16
17 37 fused and rings when struck, or devitrification to clay), and grain-size when compared with
18
19 38 surrounding lithologies. But, these deposits often are overlooked because they are relatively thin
20
21
22 39 (mm–cm) and discontinuous. Yet, when identified and sampled, often provide temporal insight.

23 24 40 4.3.1.1 Eastern Cape Province

25
26
27 41 Volcanogenic sediments are more common in the Eastern Cape localities where they
28
29 42 occur in the form of silicified ash (e.g., porcellanite; Gastaldo et al., 2018) or, more often, as a
30
31
32 43 devitrified claystone (tuffite; Gastaldo et al., 2014, 2021, unpublished). Analytical results of all
33
34 44 horizons studied, to date, indicate that these deposits are Lopingian in age (Fig. 2). The youngest
35
36
37 45 Changhsingian airfall deposits are found in close stratigraphic proximity to megafloral and
38
39 46 microfloral assemblages on Tweefontein and Blaauwater farms. But, caution is advised on
40
41
42 47 interpreting an age for a succession in which tuffites occur because older, reworked
43
44 48 Wuchiapingian tuffs occur as trough fills in fluvial crossbed sets situated stratigraphically above
45
46
47 49 these airfall horizons (Gastaldo et al., 2021). In the absence of, or in conjunction with, U-Pb
48
49 50 geochronometric constraints based on one or more suites of zircon crystals, rock magnetic data
50
51
52 51 can provide broader temporal constraints (see 4.3.2).

53 54 52 4.3.1.2 Free State Province

55
56
57 53 In contrast to volcanogenic beds in the Eastern Cape, only devitrified claystone has been
58
59

1
2
3
4 54 encountered in the Free State at one locality, to date. A discontinuous, thin, cm-thick devitrified,
5
6
7 55 light gray clay occurs on farm Nooitgedacht from which ~1000 pristine, euhedral zircon grains
8
9 56 were recovered from ~800 g of the unit (Gastaldo et al., 2020a). Pristine zircon differs from
10
11
12 57 detrital zircon recovered from siltstone directly below and above the ash. Zircon recovered from
13
14 58 the ash exhibit long or short prismatic, equant, or multi-faceted grains that are translucent; in
15
16
17 59 contrast, detrital zircons have a wide variation in grain size, morphology, and color, and exhibit
18
19 60 variable surface abrasion and rounding. A suite of 13 pristine zircon grains analyzed by U-Pb
20
21
22 61 CA-ID-TIMS gives a latest Changhsingian age of 252.24 ± 0.11 Ma (Gastaldo et al., 2020a) to
23
24 62 the airfall ash, which is situated ~5 m above the vertebrate-defined PTB of Botha et al. (2020).

25
26
27 63 Botha et al. (2020, p. 6) report results of U-Pb LA-ICP-MS analyses on a suite of detrital
28
29 64 zircon grains recovered from a sandstone low in the Spitskop section below their vertebrate-
30
31
32 65 defined, mass-extinction event. The largest modal peak is latest Permian with all dates reported
33
34 66 with uncertainties of several million years, which is a consequence of this analytical technique.
35
36
37 67 An early Triassic U-Pb ID-TIMS age of 251.7 ± 0.3 Ma, based on the five youngest detrital
38
39 68 zircons, also is reported from a siltstone (Botha et al., 2020, their table 2 and fig. 3) ~3 m below
40
41
42 69 their boundary extinction event. Neither analytical data of these five grains, nor any U-Pb ID-
43
44 70 TIMS data of this sample suite, are provided either in their text or supplemental data. Gastaldo et
45
46
47 71 al. (2020a) noted that this earliest Triassic, detrital zircon, maximum age for their upper
48
49 72 *Daptocephalus* AZ postdates the end-Permian event in the oceans (251.941–250.880 Ma;
50
51
52 73 Burgess et al., 2014). The terrestrial extinction event identified in coastal plain deposits of
53
54 74 Eastern Australia is dated to begin at 252.31 ± 0.07 Ma and lasted ~100 ka (Mays et al., 2020;
55
56
57 75 and others).

4.3.2 Magnetostratigraphy

Rock magnetic properties, if not reset by younger intrusive activity, can provide insight into the broad timing of when landscapes developed. When attempting to discern time, magnetic polarity data obtained from closely spaced stratigraphic horizons, either by drilling or oriented sampling of siltstone (Gastaldo et al., 2018, 2021), provide a magnetostratigraphy that can be evaluated in several ways. First, the thickness of the stratigraphic succession in which either a normal or reverse polarity magnetozone is documented produces a comparative record for an estimate of the duration of each. Although there is wide variance in the span of a chron over Earth history, the average magnetozone duration has been determined to be ~180 ka (Lowrie and Kent, 2004). Hence, normal and reverse magnetozones of a similar thickness in a fully continental succession roughly could be considered time equivalents, with caveats. When a magnetozone is truncated by an erosional unconformity, though, and overlain by rocks exhibiting the opposite magnetic signal, time is missing. The actual amount of missing time is difficult to discern. But, a thin magnetozone of a few meters thickness underlying the erosional unconformity certainly represents significantly more missing time than a thicker underlying magnetozone extending over decameters (Fig. 9). Secondly, correlative stratigraphic sections over distances of only several kilometers may not preserve the same magnetostratigraphic record, especially if thin, truncated magnetozones characterize the succession. Where one or more thin magnetozones, truncated at their upper boundary, may be present in one measured section, one or more of these intervals may be absent in a correlative section (see Gastaldo et al., 2021). Both of these factors influence the interpretation of whether a “continuous” stratigraphic record is present in any specific part of a basin and the biological trends preserved therein.

1
2
3
4 498 4.3.2.1 Eastern Cape Province
5

6
7 499 Rocks in the Old Lootsberg Pass section record the presence of four normal polarity and
8
9 300 three reverse polarity magnetozones (Fig. 10). All normal polarity intervals extend over tens of
10
11 501 meters; in contrast, reverse polarity intervals are short and truncated by erosional unconformities.
12
13
14 502 Only ~1.5 km to the east in the Tweefontein¹ section, two normal and one reverse polarity
15
16 503 magnetozones are identified (Gastaldo et al., 2021, fig. 19), where the latter occurs in a
17
18
19 504 stratigraphic position that is below that of the Old Lootsberg Pass reverse magnetozones. The
20
21
22 505 interval in which the upper reverse polarity magnetozones may occur, if not eroded away, was not
23
24 506 sampled due to logistics. Only a single normal polarity magnetozones is documents in the rocks ~
25
26
27 507 4 km farther to the east in the Tweefontein² section, the thickness of which encompasses both the
28
29
30 508 lower and upper reverse polarity magnetozones at Old Lootsberg Pass. Hence, depending on
31
32
33 509 where sections are measured and sampled for rock magnetic properties, very different
34
35
36 510 impressions and interpretations of time are manifested over a short lateral distance in-and-around
37
38 511 these classic localities.

39 512 Rocks at both Old and New Wapadsberg Pass have been remagnetized by dolerite
40
41
42 513 intrusions with the emplacement of the Jurassic Karoo-Ferrar Large Igneous Province (LIP). It
43
44 514 has not been possible to recover their primary magnetization. Approximately 3 km to the
45
46
47 515 northwest of these classic sites, though, Akatakpo et al. (2022) report the rock magnetic
48
49
50 516 properties for two measured sections on farm Pienaarsbaaken. Here, two normal and one reverse
51
52 517 polarity magnetozones are encountered. The reverse magnetic polarity magnetozones occurs near
53
54
55 518 the base of the 180 m section (Table 1) and is bracketed by normal polarity intervals. The upper
56
57 519 normal polarity intervals are interpreted to be of Changhsingian age based on an associated
58
59
60
61
62
63
64
65

1
2
3
4 20 palynoflora (Gastaldo et al., 2018).
5

6 7 21 4.3.2.2 Free State Province 8

9 22 Rock magnetic properties of strata in the classic Bethel farm site have allowed for the
10
11
12 23 development of a magnetostratigraphy in three measured sections, correlated across the valley,
13
14 24 encompassing > 100 m in thickness (Gastaldo et al., 2019, 2020). Two intervals sampled in close
15
16
17 25 proximity to dolerite intrusives show polarity resets, with these effects documented only within
18
19 26 several meters of the contact with the surrounding sedimentary units. Two normal and one
20
21
22 27 reverse polarity magnetozone are identified, wherein the vertebrate-defined PTB (=End Permian
23
24 28 Extinction; Ward et al., 2000, 2005; Retallack et al., 2003; Smith and Botha, 2014; Viglietti et
25
26
27 29 al., 2022) occurs in a reverse polarity interval (Gastaldo et al., 2019, fig. 5). We note that the
28
29 30 marine-defined PTB occurs in a normal polarity magnetozone (Shen et al., 2019). To date, there
30
31
32 31 are no constraining geochronometric data from these sites. In contrast, the magnetostratigraphy
33
34 32 reported from the Loskop section on farm Nooitgedacht, constrained by a U-Pb age date (see
35
36
37 33 4.3.2.1; Gastaldo et al., 2020), occurs in a normal polarity magnetozone (see: 4.3.1.2). The upper
38
39 34 bounding surface of the magnetozone is erosional and overlain by a fluvial sandstone body with a
40
41
42 35 basal pedogenic conglomerate-lag deposit.
43

44 36 **4.4 Paleobotanical Assemblages in Geochronologic and Magnetostratigraphic context** 45

46
47 37 The oldest *Glossopteris*-dominated megafloras and microfloras exposed in the Eastern
48
49 38 Cape Province are preserved in early Changhsingian beds on Tweefontein¹. These lie below an
50
51
52 39 age of 253.48 ± 0.15 Ma at an equivalent stratigraphic position in the correlative Old Lootsberg
53
54 40 Pass section (Fig. 10; Gastaldo et al., 2021). Both age-constrained beds are in an unequivocal
55
56
57 41 normal polarity magnetozone which, in the Karoo, falls in a long, reverse polarity magnetozone
58
59

1
2
3
4 42 of the global composite of Hounslow and Balabanov (2016). Currently, there is neither a reliable
5
6
7 43 age constraint on, nor a magnetostratigraphic context for, the paleosol leaf-litter horizon exposed
8
9 44 along New Wapadsberg Pass (Prevec et al., 2010; Gastaldo et al., 2014). This is because tuffite in
10
11
12 45 close association with this plant bed yielded only a few detrital zircon grains and rock magnetic
13
14 46 properties are reset by dolerite intrusions. Gastaldo et al. (2018; unpublished) note that the three
15
16
17 47 youngest grains yielded ages of 253.6 ± 0.7 Ma, 253.2 ± 0.3 Ma, and 252.03 ± 0.4 Ma. But,
18
19 48 without a sufficient number of high-resolution zircon analyses from pristine grains, with which a
20
21
22 49 concordia plot can be developed, the age of the paleosol litter remains constrained to the
23
24 50 Changhsingian by palynostratigraphy (*D. parvithola* zone; Gastaldo et al., 2021).

25
26
27 51 Younger, latest Permian assemblages are constrained by U-Pb ages in the Eastern Cape
28
29 52 and Free State provinces. The *Glossopteris*-dominated mega- and microfloral assemblages at Old
30
31
32 53 Lootsberg Pass (Gastaldo et al., 2017) lie ~65 m above an age of 252.43 ± 0.19 Ma in the
33
34 54 correlative Tweefontein² section (Fig. 10; Gastaldo et al., 2021). These assemblages are also in a
35
36
37 55 normal polarity magnetozone that likely falls in the 1n.2n magnetozone (LT1n chron), which
38
39 56 spans the PTB, of the global composite of Hounslow and Balabanov (2016). Beds in which
40
41
42 57 *Glossopteris* leaves are preserved higher in the Old Lootsberg Pass section (Gastaldo et al., 2017)
43
44 58 occur in a different normal polarity magnetozone. This interval overlies a very short, reverse
45
46
47 59 polarity magnetozone that was truncated by erosion and landscape degradation (Fig. 9); this
48
49
50 60 relationship is not recognized in the latest Permian, global composite by Hounslow and
51
52 61 Balabanov (2016). These authors recognize the presence of a reverse polarity magnetozone 1n.1r
53
54 62 in the lower Triassic above the long normal magnetozone that encompasses the PTB. To date, we
55
56
57 63 have not encountered any volcanogenic deposit in close proximity to the Old Lootsberg Pass
58
59
60
61
62
63
64
65

1
2
3
4 564 floras that allow us to geochronometrically constrain their age. This is not the case for floras at
5
6
7 565 Nooitgedacht.

8
9 366 A latest Permian age of 252.24 ± 0.11 Ma in the Free State Province at Nooitgedacht
10
11
12 567 (Gastaldo et al., 2020a) overlies the *Glossopteris* floras reported by Botha et al. (2020). The U-Pb
13
14 568 age also lies in the 1n.2n normal polarity magnetozone of the LT1n Chron of Hounslow and
15
16
17 569 Balabanov (2016). Similarly, the presence of a palynological assemblage assigned to the *D.*
18
19 570 *parvithola* zone, a few meters above the volcanogenic deposit, also lies in the same normal
20
21
22 571 polarity magnetozone (Fig. 2). But, this succession is truncated by an erosional contact with an
23
24 572 intraformational conglomerate at the base of an overlying sandstone-channel. A younger
25
26
27 573 microfloral assemblage, assigned to the *Playfordiaspora crenulata* palynozone, in which
28
29
30 574 glossopterid pollen continues to comprise up to 40% of the assemblage (Mays et al., 2021), was
31
32
33 575 recovered from siltstone in trough crossbed fills (Fig. 2; Gastaldo et al., 2020). The upper
34
35
36 576 boundary of this palynozone in Eastern Australia recently has been extended from the PTB
37
38
39 577 (Mays et al. 2020) to the Griesbachian–Dinerian boundary (250.4 Ma; Mays et al., 2021). To
40
41
42 578 date, we have neither geochronometric nor paleomagnetic data for this part of the Nooitgedacht
43
44
45 579 section to better constrain the age of the *P. crenulata* microfloral assemblage. The same is true
46
47
48 580 for the spore-and-pollen assemblage recovered from Donald 207 farm.

49
50 581 Barbolini et al. (2018) first reported, and Gastaldo et al. (2019) reaffirmed, a microfloral
51
52
53 582 assemblage on Donald 207 farm in close stratigraphic proximity to what other authors have
54
55
56 583 termed the *Lystrosaurus* bone bed, interpreted to represent vertebrate recovery in the very earliest
57
58
59 584 Triassic (e.g., Viglietti et al., 2013; Smith and Botha, 2014; Smith et al., 2022). The
60
61
62 585 palynoassemblage is assigned to the *Protohaplopinus microcorpus* palynozone which, at the time
63
64
65

1
2
3
4 386 was interpreted to postdate the disappearance of *Glossopteris* in the latest Permian of Australia
5
6
7 387 (Mays et al., 2020; Vajda et al., 2020). The presence of *Reduviasporites* (Fig. 8L), an element of
8
9 388 the Free State assemblage used to assign the assemblage to the *P. microcorpus* zone (Gastaldo et
10
11
12 389 al., 2019), has been used as a proxy for the terrestrial environmental crisis in the latest Permian
13
14 390 (e.g., Looy et al., 2001). More recently, though, Mays and McLoughlin (2022) place the lower
15
16
17 391 boundary of the *P. microcorpus* palynozone at the Griesbachian–Dinerian boundary in the mid-
18
19 392 Induan at ~251.5 Ma, limited to a temporal range of ~ 200 ka. To date, we have been unable to
20
21
22 393 locate any volcanic generated deposit in any section on the farm from which a geochronometric
23
24 394 constraint can be placed on this assemblage, nor have we rock magnetic properties due to an
25
26
27 395 extensive dolerite intrusion in the shallow subsurface.

28
29 396 4.4.1 Lesson 2: Geochronometric and rock magnetic data, developed in a sequence stratigraphic
30
31
32 397 context, constrain time and biological trends in continental successions
33

34 398 Lesson 1 taught us that paleobotanical and, in fact, any continental fossil assemblage,
35
36
37 399 represents a very short temporal window into the paleobiosphere. These temporal windows are
38
39 600 dependent on a multitude of factors both operating at the time of accumulation and post
40
41
42 601 deposition. Lesson 2 has taught us that stratigraphic successions touted as “continuous”
43
44 602 continental records are not continuous, even when the presence of minor temporal diastems or
45
46
47 603 hiatuses as recognized in paleosols are acknowledged. Time is constrained best when
48
49 604 volcanogenic airfall ash deposits are encountered and a population of pristine zircon grains are
50
51
52 605 subjected to high resolution CA-ID-TIMS analyses. Recognizing the fact that volcanogenic
53
54 606 deposits are also a rarity, newly developed U-Pb LA-ICPMS techniques applied to calcite
55
56
57 607 cements in pedogenic nodules hold promise to provide age constraints on continental successions
58
59
60
61
62
63
64
65

1
2
3
4 608 where calcic paleosols occur (Davis and Rochín-Bañaga, 2021). In the absence of
5
6 609 geochronometry, the inclusion of a high-density sampling protocol to acquire rock magnetic
7
8
9 610 properties is essential. Sampling for rock magnetic data in lithologies immediately below
10
11
12 611 erosional surfaces of fluvial successions is critical in, potentially, identifying missing time. These
13
14 612 data provide the basis for the development of a magnetostratigraphy with which the proportional
15
16
17 613 representation of normal-and-reverse polarity magnetozones can be identified in the succession
18
19 614 under consideration. Only a multi-disciplinary approach can constrain the time in the rock record
20
21
22 615 and, hence, can be used to present hypotheses about the timing of events affecting the deep-time
23
24 616 biosphere.

26 617 **5. Discussion**

28
29 618 The paleontological record of a stratigraphic succession is foundational in any, and all,
30
31
32 619 interpretations of changes in the planet's biosphere during critical intervals in Earth history. First,
33
34 620 and foremost, the record is dependent on how much of the rock record is exposed, at which
35
36
37 621 paleolatitudinal site they were deposited, where those rocks are now exposed, the proportion of
38
39 622 exposed rock to the time interval under consideration, and whether or not they are accessible for
40
41
42 623 study. Wall et al. (2009) calculated that Phanerozoic sedimentary rocks comprise ~27% marine
43
44 624 carbonate, 45% marine terrigenous clastics, and ~28% continental terrigenous clastic settings,
45
46
47 625 most of the latter represent the interface of coastal plain and nearshore marine regimes. Of the
48
49 626 terrigenous clastic settings, Wall et al. (2011) estimate that the total outcrop area for the Upper
50
51
52 627 Permian (Guadalupian–Lopingian) equals ~800,000 km² whereas the Lower Triassic
53
54 628 (Induan–Olenekian) covers ~450,000 km², or 5.5% and 3%, respectively, of bedrock exposure.
55
56
57 629 The time locked away in these rocks represent 7.61 Ma and 4.7 Ma, respectively (Cohen et al.,
58
59
60
61
62
63
64
65

1
2
3
4 630 2013), and are distributed across both the southern and northern paleohemispheres in basins now
5
6
7 631 surficially exposed in South America, southern Africa, Antarctica, Central Europe, the Russian
8
9 632 platform, Siberia, India, China, and the United States. The plant-fossil record preserved in these
10
11
12 633 areas was influenced and constrained by a number of inter-related factors which vary within, and
13
14 634 across, depositional basins.

15
16
17 635 Taphonomic processes—including those related to preservation potential, biostratinomy,
18
19 636 depositional setting, sedimentation, and various geochemistries—operating during any time of
20
21
22 637 sediment-and-plant accumulation constrain the where-and-when of organic matter preservation
23
24 638 (DiMichele and Gastaldo, 2008; Locatelli, 2014). These inter-related factors portend a
25
26
27 639 discontinuous record in space and time which is due to the inherent nature of preserving “soft”
28
29
30 640 non-mineralized plant tissues. Subsequent tectonic and surficial processes operating over various
31
32
33 641 time scales, ranging from 10s of thousands to 10s of millions or more years, will modify the
34
35
36 642 potential record that can be recovered. These post-depositional, long-term processes also reduce
37
38
39 643 the scope and number of fossiliferous horizons from which interpretations can be made (Gastaldo
40
41
42 644 and Demko, 2011). Hence, it is not parsimonious to accept a stratigraphy on its face value when
43
44
45 645 evaluating any biological or geochemical trend preserved therein. Only a high spatial and
46
47
48 646 temporal resolution record can provide the insights needed when considering Earth Systems
49
50
51 647 perturbation and ecosystem response of various scales in, across, and between correlative basins.

52
53
54 648 To state the obvious, Earth’s paleontological record from which ecological patterns are
55
56
57 649 discerned is restricted to a very small proportion of sedimentary successions spread over, and
58
59
60 650 clustered, in geologic time. It is demonstrated, unequivocally, that marine diversity, as well as
61
62
63 651 ecological, turnover, and extinction patterns, are contingent upon the sequence stratigraphic
64
65

1
2
3
4 652 framework from which invertebrate assemblages are collected and assessed (Patkowsky and
5
6
7 653 Holland, 2012). In the marine record, turnover-and-extinction patterns are not randomly
8
9 654 distributed. The abrupt transitions in the invertebrate record are intricately tied to both
10
11
12 655 unconformities of various nature as well as the spatial distribution of condensed stratigraphic
13
14 656 intervals in a basin (Holland and Patkowsky, 2015). Although the same principles apply in
15
16
17 657 coastal and fully continental successions (DiMichele and Gastaldo, 2008; Gastaldo and Demko,
18
19 658 2011), these fundamental constraints often are discounted or overlooked for any number of
20
21
22 659 reasons. Such reasons are not limited to, but may include: (1) the availability of outcrop, both as
23
24 660 a consequence of the structural attitude of the rock and the extent of cover, limiting exposure; (2)
25
26
27 661 the reliance on a single measured or composite stratigraphic section, or a small number of
28
29 662 measured sections in close geographic proximity, in any locality from which to interpret regional
30
31
32 663 or global biological patterns; (3) the assumption that the paleontological record, and the rocks in
33
34 664 which they are preserved, in one area are temporally equivalent to patterns encountered in other
35
36
37 665 regions that may be tens, hundreds, or thousands of kilometers distant without the presence of an
38
39 666 unequivocal datum, independent of biostratigraphic presupposition, on which correlation can be
40
41
42 667 made; and (4) the absence of a multi-disciplinary approach. Such a multi-disciplinary approach–
43
44 668 employing rock magnetic properties, geochemistry, and geochronometry, where possible–has
45
46
47 669 been used in the Karoo Basin to resolve time and allow for biological patterns to be better
48
49 670 evaluated. All of these factors play a role in the paleontological, and particularly the
50
51
52 671 paleobotanical, record of the upper Permian and Lower Triassic rocks of the Karoo Supergroup.
53
54 672 And, contrary to an interpretation that these rocks represent a “continuous” succession with the
55
56
57 673 presence of only minor hiatuses (e.g., Smith, 1995; Viglietti et al., 2021), our studies over the
58
59
60
61
62
63
64
65

1
2
3
4 674 past two decades have shown this belief to be an oversimplification (Fig. 10; see 4.4.1 Lesson 2).
5
6
7 675 The paleontological record in the Balfour and Katberg formations is more complex than what is
8
9 676 proposed, and accepted, in the published literature.
10

11 677 **5.1 Paleobotanical assemblages in space and time**

12 678 5.1.2 Spatial relationships of plant-fossil assemblages

13
14
15
16
17 679 A taphonomic window exists under which subsurface and subaerial plant parts can
18
19 680 potentially be added to, and preserved in, the fossil record. The criteria required for preservation
20
21
22 681 vary within landscapes and across latitudinal zones at any, and all points in time. In fully
23
24 682 continental basins where no marine influence on sedimentation is known, such as the Beaufort
25
26 683 Group of the Karoo Basin (Fig. 2), there is a limited spectrum of depositional environments
27
28
29 684 where there existed a potential for preservation resulting in a limited number of fossil-plant
30
31
32 685 assemblages. The lowest plant-preservation potential exists in soils where both physical and
33
34 686 biological processes continuously operate on the substrate across various climatically influenced
35
36
37 687 pedotypes. Pedogenic modifications of floodplain (interfluvial) sediments include, but are not
38
39 688 limited to: hydrolysis (weathering of feldspathic minerals to clay), calcification (CaCO_3
40
41
42 689 enrichment and the precipitation of calcite-cemented nodules), salinization (precipitation of salts
43
44 690 in the soil profile), and gleization (organic matter accumulation and iron reduction where water
45
46
47 691 tables are high; Sheldon and Tabor, 2013). Bioturbation and utilization of soil biomass by
48
49 692 invertebrates (e.g., *Katbergia*; Gastaldo and Rolerson, 2008) and vertebrates (e.g., Bordy et al.,
50
51
52 693 2011), and phytoturbation of sediments via successive generations of roots, in conjunction with
53
54 694 climate and rainfall patterns over the time span of pedogenesis, change both surficial and the
55
56
57 695 pore-water geochemistries such that surficial litters decay and are recycled rapidly (e.g., Gastaldo
58
59
60
61
62
63
64
65

1
2
3
4 696 and Staub, 1999). Under exceptional circumstances, vertical and subhorizontal rooting structures
5
6
7 697 may be preserved either as adpressions or clay-lined impressions (Retallack, 1988), or act as
8
9 698 nuclei for calcite-nodule precipitation in which roots are preserved (e.g., Gastaldo et al., 2014).
10
11
12 699 When present, such rooting structures represent the final phase of soil development before the
13
14 700 landscape was rapidly removed from the soil-air interface and buried at a depth beyond the
15
16
17 701 influence of renewed surficial pedogenic processes. Such a rapid, regional base-level change
18
19 702 generally is tectonically influenced and accompanied by increased sedimentation as new
20
21
22 703 accommodation is formed in response to changing depocenters and fluvial gradients (Gastaldo
23
24 704 and Demko, 2011). In essence, marine obrution deposits (Brett, 1990) can be considered
25
26
27 705 equivalents to paleosols in which subterranean and, especially in exceptional circumstances, O-
28
29 706 horizons are well preserved (e.g., Gastaldo et al., 2014).
30

31
32 707 Soils constitute the greatest volume and aerial distribution of sedimentary environments
33
34 708 across any continental landscape. When mudrock paleosols constitute the greatest proportion of
35
36
37 709 the stratigraphic record, as they do in the Karoo succession, encountering any fossil-plant
38
39 710 assemblage in rocks representing these settings is near impossible. To date, we have encountered
40
41
42 711 only a single paleosol in the Balfour Formation at Wapadsberg Pass wherein both a macroflora
43
44 712 (subterranean and leaf-litter assemblages) is preserved along with a microfloral assemblage
45
46
47 713 (Prevec et al., 2010; Gastaldo et al., 2014). This single occurrence represents 0.03% of our upper
48
49 714 Permian–lower Triassic stratigraphic record (Table 2). Adpressions and palynology are preserved
50
51
52 715 in other depositional environments, and preservation in these settings account for a higher
53
54 716 percentage of paleobotanical assemblages in the Balfour and Katberg formations.
55

56
57 717 Rivers dissect the floodplain landscape on which soils develop. Sediment accumulation
58
59
60
61
62
63
64
65

1
2
3
4 18 during times of pedogenesis occurs as bedload deposits that include channel lags and overlying
5
6
7 19 barforms of various configuration where plant debris, transported as suspension load, may settle
8
9 20 on bedding planes of low-velocity bedforms (lamination, trough fills, planar and trough cross
10
11
12 21 beds and bedsets). If grain size is small (very fine sand [125–62.5 μm] and silt [62.5–3.9 μm]),
13
14 22 sediment supply is periodically high, and sediment accumulation is coincident at the time of
15
16
17 23 phytoclast emplacement, plant debris may be buried increasing its preservation potential. Often,
18
19 24 though, fluctuations in pore-water geochemistry (oxygen, redox, etc.), as well as fungal and
20
21
22 25 bacterial activity, just below the sediment-water interface promote the decay of buried detritus. In
23
24 26 most instances, decay of these organic drapes results in an organic lamination in which only the
25
26
27 27 most recalcitrant axes may be identifiable. Such phytoclast fields (e.g., comminuted or dispersed
28
29 28 plant detritus) are a common feature of many, but not all, fluvial deposits. Their presence or
30
31
32 29 absence is a function of fluvial discharge rates that operated at the time of sediment transport and
33
34 30 deposition. The rates under which sediment accumulated can be broadly ascertained by the array
35
36
37 31 of primary sedimentary structures found in channel deposits. The higher the discharge
38
39 32 rates—reflected in the presence of trough cross, plane laminated, and massive bedding—the greater
40
41
42 33 reworking of bedload and physical fragmentation of previously emplaced debris in the traction
43
44 34 load (Gastaldo, 1994). Without consideration of the dominant primary structure in river deposits,
45
46
47 35 one can be lead to the impression that adjacent floodplains were devoid of vegetation when, in all
48
49 36 probability, the absence of phytodebris was a function of discharge energy. Beaufort Group (Fig.
50
51
52 37 2) river deposits are dominated by trough cross beds of various scale in which there are few
53
54 38 examples of phytoclast fields draping bedding (Gastaldo et al., 2021). This is in stark contrast to
55
56
57 39 Upper Permian and Lower Triassic fluvial deposits in the Bogda Mountains, Xinjiang Province,
58
59
60
61
62
63
64
65

1
2
3
4 740 western China. Here, phytoclast fields (including palynomorphs) are the most commonly
5
6
7 741 preserved plant assemblage found throughout river deposits dominated by low-angle crossbeds
8
9 742 (Gastaldo et al., in press). Although phytoclast fields may preserve identifiable plant detritus
10
11
12 743 (Gastaldo et al., 2005), higher preservation potential exists for plant parts transported into
13
14 744 standing bodies of water (abandoned and oxbow channels, open or closed lakes) that are enclosed
15
16
17 745 in floodplain soils.

18
19 746 Not all standing bodies of water have the same preservation potential of plant debris
20
21
22 747 introduced into a depression in any landscape. Preservation requires sufficient water depth and
23
24 748 amenable bottom-water geochemistries, which may promote the development of surficial
25
26
27 749 biofilms (Dunn et al., 1997) or entombment in microbial mats (Kerp et al., 1996; Iniesto et al.,
28
29 750 2018). In most instances, preservation of allochthonous assemblages requires a higher
30
31
32 751 suspension-load sedimentation rate wherein organic decay is impeded, rather than promoted.
33
34 752 Surface-lake waters are thermally stratified and well oxygenated, with dysoxia (0.3–2 mg/l) or
35
36
37 753 anoxia (0–0.2 mg/l) generally restricted to bottom waters at depths below the oxygen minimum
38
39 754 zone (OMZ). In the case of modern lakes, the OMZ is tens of meters below the water-air
40
41
42 755 interface where invertebrate activity is restricted or curtailed at the sediment-water interface and
43
44 756 shallow subsurface. And, the depth of the OMZ in a lake is influenced by its geographical and
45
46
47 757 latitudinal position in the past, as well as seasonality. Bedded litters and plant assemblages in
48
49 758 laminated beds are indicative of their residency at the bottom of a standing water body below the
50
51
52 759 OMZ, where the taphonomically active zone (TAZ) of invertebrate activity was suppressed at the
53
54 760 time of emplacement of both the plant debris and entombing sediment. Seasonal changes and/or
55
56
57 761 oscillations in bottom-water geochemistry (oxygenation, temperature, redox, etc.) will reinstate
58
59
60
61
62
63
64
65

1
2
3
4 762 conditions for reactivation of invertebrate activity in bottom sediments, recycling organic matter
5
6
7 763 both at the benthic-water interface and shallow subsurface. Even if the number of lakes in an area
8
9 764 was high, and lakes were spread across one or more interfluvial landscapes, conditions in each
10
11
12 765 lake would have differed at various points in time restricting the site(s) in which plants could
13
14 766 have been preserved. Hence, coeval settings would not have had the same potential to preserve
15
16
17 767 plant debris, which limits the probability of encountering a fossil assemblage in surficial
18
19 768 exposures of these facies, particularly where outcrops are limited or found to be two dimensional.
20

21 22 769 5.1.2 Lesson 3: Spatial distribution of paleobotanical assemblages

23
24 770 Plant-fossil assemblages are neither distributed equally within or across correlative
25
26
27 771 sections. Soft-tissue preservation requires a multitude of co-occurring factors which, at the most
28
29 772 fundamental level, requires: (1) a depositional site in which plant-and-sediment accumulation
30
31
32 773 occurs contemporaneously; (2) the isolation of plant debris under geochemical conditions
33
34 774 conducive to constraining decay and increasing the potential for its conservation; and (3) the
35
36
37 775 subsequent maintenance of that landscape allowing for its retention in the stratigraphic
38
39 776 succession (Behrensmeyer et al., 2000; DiMichele and Gastaldo, 2008). Additionally, there is the
40
41
42 777 low probability of encountering these facies in non-contiguous outcrops because of their
43
44 778 geographic distribution in and across the original landscape. As demonstrated in the Karoo Basin,
45
46
47 779 with similar data coming from the Hami-Turpan Basin, China (Gastaldo et al., in press),
48
49 780 megafloreal assemblages constitute a very small proportion of lithostratigraphies in correlative
50
51
52 781 sections. Hence, our understanding of vegetation in this part of the Karoo succession is
53
54 782 contingent on a limited number of fossiliferous beds that, generally, are preserved over a rock
55
56
57 783 thickness of a few decimeters, and are restricted in outcrops available for study at the present.
58
59
60
61
62
63
64
65

1
2
3
4 784 Plant-rich deposits represent very limited spatial “windows” into the (paleo)biosphere and are
5
6
7 785 biased toward plant debris sourced from vegetation growing in soils marginal to depositional
8
9 786 settings. This is true in all fully continental basins.

11 12 787 5.2 Temporal relationships of plant-fossil assemblages

13
14 788 Various perspectives about the timing of plant-rich assemblages in the Beaufort Group
15
16
17 789 can be advanced. Here, we focus on the record of well-preserved plant assemblages (Figs. 10, 11)
18
19 790 and disregard the geographical distribution of potential depositional settings across that
20
21
22 791 landscape (see 5.1.2). Gastaldo and Demko (2011) proposed that plant preservation has a higher
23
24 792 probability to be incorporated and preserved in the stratigraphic record during the initial phases
25
26
27 793 of landscape build up, or aggradation, in an active depocenter following a resetting of local
28
29 794 and/or regional base level (see full discussion in Gastaldo et al., 2020c). This is because
30
31
32 795 sediment-accumulation rates are highest during this initial phase of transport and deposition. A
33
34 796 coincidence of high sediment supply and depositional rates, along with biomass contribution
35
36
37 797 from riparian (river and lake side) vegetation, results in the highest probability that plants will be
38
39 798 buried and preserved in these deposits. Their conservation is the result of rapidly filling
40
41
42 799 accommodation, embedding leaf litters in sediment that is unaffected by bioturbation (Figs. 4A,
43
44 800 B). The residency times of phytodebris at the sediment-water interface are short, where there is a
45
46
47 801 suppression of the TAZ, either via high suspension-load sedimentation or bottom-water
48
49 802 geochemistries that prevent invertebrate colonization. During the initial aggradational phase,
50
51
52 803 overbank deposition is common, interfluvial paleosols increase in thickness, and there is an
53
54 804 overall rise of the regional water table. Climate is one factor that controls aggradation wherein
55
56
57 805 poorly drained interfluvial soils are maintained under a seasonally wet climate. Changes in the
58
59
60
61
62
63
64
65

1
2
3
4 806 regional fluvial gradient, sediment supply to the drainage system, or climate shift towards more
5
6
7 807 seasonally dry or monsoonal conditions results in a slowing or cessation of floodplain
8
9 808 aggradation. As floodplain aggradation slows or ceases, pedogenesis results in more mature soil
10
11
12 809 profiles. Under these mature conditions (landscape stasis), a prevailing low sediment-
13
14 810 accumulation rate precludes the burial and isolation of phytodebris in depositional settings,
15
16
17 811 resulting in their low preservation potential. As such, there is a dearth or absence of these
18
19 812 assemblages in the final phase of an aggradational cycle, although similar depositional
20
21
22 813 environments may have existed across the landscape in which plants previously were preserved.

23
24 814 We have encountered only a few *Glossopteris*-dominated megafloral assemblages in the
25
26
27 815 Balfour Formation in aquatic settings of latest Permian age. All but one of these represents leaf-
28
29 816 litter accumulations. The one exception is the immature paleosol and O-horizon found at
30
31
32 817 Wapadsberg Pass (Prevec et al., 2010; Gastaldo et al., 2014) in the Eastern Cape Province.
33
34 818 *Glossopterid*-dominated mega- and microfloras are likely all Changhsingian in age. The
35
36
37 819 Tweefontein¹ floras (Gastaldo et al., 2017) are older than 253.48 ± 0.48 Ma, preserved in a
38
39 820 normal polarity magnetozone (Fig. 10) but are unconstrained by a geochronometric age estimate,
40
41
42 821 at present; the Wapadsberg Pass floras also are likely slightly older (sec. 4.4). In the classic
43
44 822 localities of the Eastern Cape, *Glossopteris*-dominated landscapes span at least four
45
46
47 823 magnetozones in a succession of at least 18 aggradational and degradational cycles of
48
49 824 sedimentation (Fig. 10). It is likely that the Late Permian, Eastern Cape landscapes also
50
51
52 825 underwent aggradational and degradational cycles during each reverse polarity magnetozone,
53
54 826 given the estimates of an average-magnetozone duration of ~ 180 ka (Lowrie and Kent, 2004).
55
56
57 827 The short and, at times, cryptic stratigraphic intervals in which reverse magnetozones are
58
59
60
61
62
63
64
65

1
2
3
4 828 identified, though, preclude any speculation about cycle number. In conjunction with evidence
5
6
7 829 from the Free State locality of Nooitgedacht (Botha et al., 2020; Gastaldo et al., 2020a), these
8
9 830 seasonally wet, *Glossopteris*-dominated floras ranged into the latest Permian (Fig. 11). An
10
11
12 831 unconformity occurs a few meters above the horizon from which we have obtained our U-Pb age,
13
14 832 which is overlain by a fluvial channel deposit with a basal pedogenic nodule conglomerate lag.
15
16
17 833 An overlying palynoflora conforms to the *P. crenulata* palynozone of Eastern Australia (Gastaldo
18
19 834 et al., 2020a), which is now considered to range from 252.3–251.5 Ma (Mays and McLoughlin,
20
21 835 2022). Preliminary geochronometric data from Nooitgedacht indicates an early Triassic age
22
23
24 836 assignment to the palynoflora where Mays and McLoughlin (2022) report that glossopterid-type
25
26
27 837 pollen constitute up to 40% of floras assigned to the *P. crenulata* palynozone. Pollen attributable
28
29 838 to *Glossopteris* is present in the *P. crenulata* palynozone of the Karoo (Gastaldo et al., 2021)
30
31
32 839 which also might indicate temporary persistence of the lineage into the Early Triassic in this
33
34 840 basin.

35
36
37 841 Using the Australian palynozones, Barbolini et al. (2016, 2018) placed a palynoflora from
38
39 842 the Donald 207 farm (Fig. 3) into the overlying *P. microcorpus* assemblage zone (Fig. 11). At the
40
41
42 843 time, the base of this palynozone was considered to represent catastrophic floristic turnover as a
43
44 844 consequence of the terrestrial end-Permian extinction event (Fielding et al., 2019), and Mays et
45
46
47 845 al. (2020, fig. 1) placed its upper boundary coincident with the marine event. Since then, new U-
48
49 846 Pb ages in Eastern Australia have constrained the *P. microcorpus* palynozone to the Dienarian
50
51
52 847 (latest Induan; Mays and McLoughlin, 2022). Hence, rather than it being indicative of the end-
53
54 848 Permian terrestrial crisis, the Donald 207 palynoflora (Barbolini et al., 2016; Gastaldo et al.,
55
56
57 849 2019) may be latest Induan (Fig. 11). We note that global analysis of mega- and microflora data
58
59
60
61
62
63
64
65

1
2
3
4 850 by Nowak et al. (2019) was unable to find evidence to support a mass extinction of vegetation
5
6
7 851 across the PTB. Rather, a dramatic shift in palynofloras in the Early Triassic, from the
8
9 852 Griesbachian to the Dinerian, is reported (Hochuli et al., 2016; Schneebeli-Hermann et al., 2017).
10
11
12 853 More recently, Schneebeli-Hermann (2020) proposed that Early Triassic, rather than latest
13
14 854 Permian, terrestrial microfloral assemblage trends may reflect extreme compositional ecosystem
15
16 855 shifts (extirpation) rather than outright turnover and extinction. Too few data are available in the
17
18
19 856 Karoo Supergroup with which to test these hypotheses.
20

21 22 857 5.2.1 Lesson 4: Temporal distribution of paleobotanical assemblages 23

24 858 The frequency of plant-bearing beds over a stratigraphic interval of interest will dictate
25
26 859 one's perception of biological trends in time (DiMichele and Gastaldo, 2008). Each assemblage
27
28
29 860 represents a short temporal “window” into the (paleo)biosphere, providing snapshots with which
30
31
32 861 to connect-the-dots and discern biological patterns (see sec. 5.1). The presence of *Glossopteris*-
33
34 862 dominated floras, beginning in the coals of the Vryheid Formation (279 Ma) and extending into
35
36
37 863 the latest Changhsingian, demonstrates the presence of the glossopterid biome in South Africa
38
39 864 for a duration of at least 28 My. Yet, the stratigraphy in which these assemblages are preserved,
40
41
42 865 and interpreted to span the end-Permian crisis, must also be understood. Stratigraphies must be
43
44 866 investigated at a high temporal resolution in which diastems and hiatuses are identified and,
45
46
47 867 where possible, semi-quantified before turnover, extirpation, or extinction patterns can be
48
49 868 resolved. In the case of paleontological assemblages in the Karoo's Beaufort Group, the use of
50
51
52 869 geochronological and magnetostratigraphic data in a sequence stratigraphic framework
53
54 870 demonstrates that these rocks do not represent a “continuous” record of the Permian–Triassic
55
56
57 871 transition. Rather, the rocks of the Elandsberg through Katberg interval represent highly
58
59
60
61
62
63
64
65

1
2
3
4 872 condensed successions (Figs. 10, 11), of variable thickness, where a disproportionate amount of
5
6
7 873 time is represented in sediments deposited during normal polarity magnetozones, and there is
8
9 874 significant missing time as demonstrated by the presence of short reverse polarity magnetozones.
10
11
12 875 A major unconformity exists in the Nooitgedacht section, encompassing the terrestrial end-
13
14 876 Permian crisis, making it impossible to detail biological patterns or trends that are proposed to
15
16
17 877 have occurred at that time, let alone constrain such hypotheses to a temporal resolution of 10s to
18
19 878 a 100 thousand years. Hence, it is not parsimonious to assume that fossils collected in close
20
21
22 879 stratigraphic proximity to one another record a step-by-step biological pattern constrained to a
23
24 880 short temporal scale. Neither is it parsimonious to use the stratigraphic position of a fossil
25
26
27 881 assemblage to calculate confidence intervals with which to propose a taxon's range without, first,
28
29 882 demonstrating how time is manifested in the rocks.
30

31 32 883 **6. Conclusions**

33
34 884 The demise of the *Glossopteris* flora that dominated the southern paleohemisphere
35
36
37 885 landscape for more than 26 million years—an equivalent time from the Miocene to the
38
39 886 Anthropocene—has been interpreted as the first domino to fall at the onset of the terrestrial end-
40
41
42 887 Permian crisis leading to systematic turnover and extinctions. The fossil record of the Karoo
43
44 888 Basin, South Africa, has been considered as the “golden spike” in the end-Permian narrative to
45
46
47 889 which biological trends and patterns on other continents have been compared. Here, the absence
48
49 890 of megafloral remains in upper Changhsingian rocks became the basis for interpreting
50
51
52 891 catastrophic deforestation which cascaded to vertebrate communities, and equated to the step-
53
54 892 wise extinctions documented in latest Permian oceans. Yet, the interpretation of terrestrial
55
56
57 893 patterns is dependent not only on the taphonomy of these plant assemblages and their overall
58
59
60
61
62
63
64
65

1
2
3
4 894 presence in the stratigraphic record over the interval of concern, but also on their temporal
5
6
7 895 context.

8
9 896 Glossopterid taxa dominate the Balfour Formation of the Beaufort Group where
10
11 subordinate equisetalean taxa with growth habits that include groundcover and lianas co-occur.
12 897
13
14 898 These assemblages are preserved primarily as adpressions or impressions, with the occasional
15
16
17 899 and isolated permineralized wood assemblage. All megafloral assemblages are biased to
18
19 900 seasonally wet or wetland environments where they are preserved in river barforms, abandoned
20
21
22 901 channels, and lakes in aggradational landscapes where they have the highest preservation
23
24 902 potential. These depositional settings comprised a small proportion of the overall basinal
25
26
27 903 geography at any point in time. In contrast, pedogenesis extended from river margins across the
28
29 904 adjacent floodplains, and constitute the largest aerial extent of Karoo landscapes. Paleosols
30
31
32 905 comprise the greatest proportion of the upper Permian and lower Triassic stratigraphy. Balfour
33
34 906 and Katberg formation soils range from immature (e.g., Inceptisol; Gastaldo et al., 2014) to
35
36
37 907 mature (e.g., Calcic Vertisols; Gastaldo et al., 2020b), where soils have the lowest potential for
38
39 908 plant-part preservation, as floodplain aggradation slowed in response to changes in prevailing
40
41
42 909 climate and rainfall. Microfloras evidence shifts from predominantly wetland glossopterid-
43
44 910 dominated assemblages, with little evidence for the presence of other gymnosperm taxa, to
45
46
47 911 assemblages in which peltasperms, corystosperms, voltzialean conifers and other gymnosperm
48
49 912 pollen are found in higher proportions associated with calcic Vertisols (Gastaldo et al., 2018).

50
51
52 913 The number of the depositional settings in which plants may be preserved and their
53
54 914 geographic distribution across any Karoo landscape will control the potential for being
55
56
57 915 encountered in any vertically exposed stratigraphic succession or in laterally equivalent rocks. It

1
2
3
4 16 must also be recognized that coeval depositional settings, will not have undergone the same
5
6
7 17 physical and geochemical processes, resulting in a discontinuous paleobotanical record, reducing
8
9 18 the probability of finding a bed in which plants are preserved. We have found that the
10
11
12 19 paleontological record from which ecological patterns can be discerned in the Karoo Basin, and
13
14 20 elsewhere, is restricted to a very small proportion of sedimentary successions spread over, and
15
16
17 21 clustered, in geologic time.

18
19 22 We present paleobotanical data acquired from >3780 m of measured stratigraphic section
20
21
22 23 in which permineralized wood, adpression, and microfloral assemblages are preserved in rocks
23
24 24 spanning the upper Permian and lower Triassic. Permineralized wood assemblages represent
25
26
27 25 ~0.3% of the available rock record, with adpression assemblages found in < 1% of the same
28
29
30 26 stratigraphy. Palynological assemblages have been recovered from < 1.5% of the same
31
32 27 stratigraphic interval. These data demonstrate that plant fossil assemblages represent
33
34 28 vegetational snapshots of the Changhsingian landscapes that occupied Karoo soils over a
35
36
37 29 duration of ~3 My. Megafloral assemblages serve as windows into colonized landscapes in-and-
38
39
40 30 around depositional settings, whereas microfloral assemblages represent ecologies outside of that
41
42 31 taphonomic window. These data, in conjunction with our sequence stratigraphic approach,
43
44 32 continue to demonstrate that the continental stratigraphic record is notoriously incomplete due to
45
46
47 33 the constant erosion and reworking of the land's surface. Hence, plant assemblages represent
48
49
50 34 very short temporal "windows" into the paleobiosphere when preserved.

51
52 35 The accepted paradigm of the stratigraphy spanning the uppermost Permian and
53
54 36 lowermost Triassic Karoo rocks is one of a continuous nature. Yet, temporal relationships
55
56
57 37 between units are difficult to interpret, in large part, because of a scarcity of datable sediments.
58
59
60
61
62
63
64
65

1
2
3
4 38 We demonstrate that geochronology coupled with magnetostratigraphy, and other rock-magnetic
5
6
7 39 properties, provide a temporal context for continental successions. This approach not only assists
8
9 40 in helping to resolve the overall duration of “time” that is represented in an area, but also
10
11
12 41 provides an estimate of how much “time” is missing in that rock record. We caution that
13
14
15 42 sampling regimes designed to acquire rock-magnetic properties of a succession may not result in
16
17 43 the same magnetostratigraphy when undertaken in correlative sections, even when closely
18
19 44 spaced, and especially true where one or more polarity magnetozones may thin as a consequence
20
21
22 45 of their erosion during the emplacement of an overlying aggradational landscape cycle. Hence, it
23
24 46 is not possible to rely solely on a single sampling regime in condensed, continental stratigraphic
25
26
27 47 successions, to determine a relative timing of events. As we demonstrate here, once again, the
28
29 48 Karoo succession spanning the uppermost Permian and lowermost Triassic is not a continuous
30
31
32 49 record of events in the basin. Rather, these rocks record a disproportionate amount of time in
33
34
35 50 successive landscapes. The duration of time in the Karoo succession is unequally divided. There
36
37
38 51 is a disproportionate sedimentary record, with the greatest thickness of sediment, now lithified,
39
40
41 52 deposited during chrons of normal polarity. These outweigh the proportion of time recorded in
42
43
44 53 sediment that accumulated during chrons of reverse polarity, which are found in thin intervals
45
46
47 54 that underlie erosional contacts at the base of aggradational cycles. This observation reinforces
48
49
50 55 the conclusion that the Karoo lithostratigraphy represents a succession of mainly aggradational
51
52
53 56 landscapes punctuated by degradational processes from which high-resolution biological patterns
54
55
56 57 are difficult, at best, to resolve temporally.
57
58
59
60
61
62
63
64
65

1
2
3
4
5
6
7
8
9
10
11
12
13
14
15
16
17
18
19
20
21
22
23
24
25
26
27
28
29
30
31
32
33
34
35
36
37
38
39
40
41
42
43
44
45
46
47
48
49
50
51
52
53
54
55
56
57
58
59
60
61
62
63
64
65

Declaration of competing interest

None

Acknowledgments

The authors would like to thank our colleagues who have contributed their time and effort in the advancement of South African paleobotany over this critical time in Earth history. These include: J. Neveling, Council for Geoscience, Pretoria; J. Geissman, University of Texas–Dallas; C. Looy, University of California–Berkeley; N. Tabor, Southern Methodist University, C. Labandiera, Smithsonian Institution, Washington, DC; and R. Prevec, Rhodes University, Grahamstown. We also acknowledge the efforts of Colby College undergraduate students in helping to develop our stratigraphic framework, and students in the Evolutionary Studies Institute K. Mahabeer, S. Kock, and N. Nhamutole.

Funding

Research efforts were supported, in part, by: the Council for Geoscience (South Africa); NSF EAR 0749895, 0934077, 1123570 and 1624302, and a Fulbright Scholar Award from the U.S. Department of State to RAG; and NRF-AOP 98823, DSI-NRF CoE 2017, and PAST for various grants for fieldwork to MB.

References

Aitken, G.A. 1993. Palynology of the Number Five Seam in the Witbank / Highveld coalfields. Unpublished M.Sc. Thesis, University of the Witwatersrand.

Aitken, G.A. 1994. Permian palynomorphs from the Number 5 Seam, Ecca Group, Witbank Highveld Coalfields, South Africa: *Palaeontologia africana* 31: 97-109.

Aitken, G.A. 1998. A palynological and palaeoenvironmental analysis of Permian and early

1
2
3
4
5
6
7
8
9
10
11
12
13
14
15
16
17
18
19
20
21
22
23
24
25
26
27
28
29
30
31
32
33
34
35
36
37
38
39
40
41
42
43
44
45
46
47
48
49
50
51
52
53
54
55
56
57
58
59
60
61
62
63
64
65

Triassic sediments of the Ecca and the Beaufort groups, Northern Karoo Basin, South Africa. Unpublished Ph.D. Thesis, University of the Witwatersrand.

Akatakpo, S., Geissman, J.W., Gastaldo, R.A., Neveling, J., Looy, C., 2022, Paleomagnetism and rock magnetism of Upper Permian/Lower Triassic Beaufort Group Strata and early Jurassic mafic sills from Pienaarsbaaken section, eastern Karoo Basin, South Africa. Am. Geol. Union, Abstr.

Anderson, J.M., Anderson, H.M. 1985. Palaeoflora of southern Africa. Prodomus of southern African megafloras Devonian to Lower Cretaceous. A.A. Balkema, Rotterdam, The Netherlands, 423 p.

Angielczyk, K., Roopnarine, P., Wang, S. 2005. Modeling the role of primary productivity disruption in end-Permian extinctions, Karoo Basin, South Africa. The Nonmarine Permian. New Mex. Mus. Nat. Hist. Sci. Bull. 30. 16-23.

Bamford, M.K. 1999. Permo-Triassic fossil woods from the South African Karoo Basin. Palaeont. afr. 35. 25–40.

Bamford, M.K. 2000. Fossil woods of Karoo aged deposits in South Africa and Namibia as an aid to biostratigraphic correlation. J Afr. Earth Sci. 31. 119-132.

Bamford, M.K. 2004. Diversity of the Woody Vegetation of Gondwanan Southern Africa. Gond. Res. 7. 153-164.

Bamford, M.K., Phillippe, M. 2001. Gondwanan Jurassic–Early Cretaceous homoxyulous woods: a nomenclatural revision of the genera with taxonomical notes: Rev. Palaeobot. Palynol. 113. 287–297.

Bamford, M.K., Cairncross, B., Lombard, H. 2020. Silicified fossil woods from the Late Permian

- 1
2
3
4
5 Middleton Formation, Beaufort Group, Eastern Cape Province, South Africa and their
6
7
8
9
10
11
12
13
14
15
16
17
18
19
20
21
22
23
24
25
26
27
28
29
30
31
32
33
34
35
36
37
38
39
40
41
42
43
44
45
46
47
48
49
50
51
52
53
54
55
56
57
58
59
60
61
62
63
64
65
- 1002 Middleton Formation, Beaufort Group, Eastern Cape Province, South Africa and their
1003 palaeoenvironmental significance. *S. Afr. J. Geol.* 123. 465–478. doi:
1004 <https://doi-org.colby.idm.oclc.org/10.25131/sajg.123.0036>
- 1005 Barbolini, N., Bamford M.K., Rubidge B. 2016. Radiometric dating demonstrates that Permian
1006 spore pollen zones of Australia and South Africa are diachronous. *Gond. Res.* 37.
1007 241–251.
- 1008 Barbolini, N., Rubidge, B., Bamford, M.K. 2018. A new approach to biostratigraphy in the Karoo
1009 retroarc foreland system: utilizing restricted-range palynomorphs and their first
1010 appearance datums for correlation. *J. Afr. Earth Sci.* 140. 114–133.
- 1011 Behrensmeier, A.K., Kidwell, S.M., Gastaldo, R.A. 2000. Taphonomy and paleobiology.
1012 *Paleobiology.* 26. 103–147.
- 1013 Blumenkemper, P., Kerp, H., Bomfleur, B. 2019. A treasure trove of peculiar Permian plant
1014 fossils. *PalZ*, 94. 409–412.
- 1015 Bordy, E.M., Prevec, R. 2008. Sedimentology, palaeontology and palaeo-environments of the
1016 Middle (?) To Upper Permian Emakwezini Formation (Karoo Supergroup, South Africa.
1017 *S. Afr. J. Geol.* 111. 429-456. doi:10.2113/gssajg.111.4.426 (add to text and citations)
- 1018 Bordy, E.M., Prevec, R. 2015. Lithostratigraphy of the Emakwezini Formation (Karoo
1019 Supergroup), South Africa. *S. Afr. J. Geol.* 118. 307-310. doi:10.2113/gssajg.118.3.307.
- 1020 Bordy, E.M., Hancox, P.J., Rubidge, B.S., 2005. The contact of the Molteno and Elliot
1021 formations through the main Karoo Basin, South Africa: a second-order sequence
1022 boundary. *S. Afr. J. Geol.* 108. 351-364.
- 1023 Bordy, E.M., Sztanó, O., Rubidge, B.S., Bumby, A. 2011. Early Triassic vertebrate burrows from

1
2
3
4
1024 the Katberg Formation of the south-western Karoo Basin, South Africa. *Lethaia*. 44.
5
6
7
1025 33–45.
8
9
1026 Bordy, E.M., Abrahams, M., Sharman, G.R., Viglietti, P.A., Benson, R.B.J., McPhee, B.W.,
10
11
1027 Berrett, P.M., Sciscio, L., Condon, D., Mundil, R., Rademan, Z., Jinna, Z., Clark, J.M.,
12
13
14
1028 Suarez, C.A., Chapelle, K.E.J., Choiniere, J.N., 2020. A chronostratigraphic framework
15
16
1029 for the upper Stormberg Group: Implications for the Triassic-Jurassic boundary in
17
18
19
1030 southern Africa. *Earth Sci. Rev.* 203. 103120.
20
21
1031 <https://doi.org/10.1016/j.earscirev.2020.103120>.
22
23
24
1032 Botha, J., Smith, R.M.H. 2020. Biostratigraphy of the *Lystrosaurus declivis* Assemblage Zone
25
26
1033 (Beaufort Group, Karoo Supergroup), South Africa. *S. Afr. J. Geol.* 123.2. 207–216.
27
28
1034 doi:10.25131/sajg.123.0015
29
30
31
1035 Botha, J., Huttenlocker, A.K., Smith, R.M.H., Prevec, R., Viglietti, P., Modesto, S.P. 2020. New
32
33
1036 geochemical and palaeontological data from the Permian-Triassic boundary in the South
34
35
36
1037 African Karoo Basin test the synchronicity of terrestrial and marine extinctions. *Palaeo*
37
38
1038 *Palaeo* 540, 109467.
39
40
41
1039 Brett, C.E. 1990. Ostracod deposits, *in* Briggs, D.E.G., Crowther, P.R., eds. *Palaeobiology: A*
42
43
1040 *Synthesis*. Blackwell Scientific Publications, Oxford, London. 239–243.
44
45
46
1041 Bull, W.B. 1991. *Geomorphic responses to climatic change*. Oxford, UK: Oxford University
47
48
1042 Press. 326 p.
49
50
51
1043 Burgess, S.D., Bowring, S., Shen, S.-Z. 2014. High-precision timeline for Earth's most severe
52
53
1044 extinction. *Proc. Nat. Acad. Sci. USA.* 111. 3316–3321. <https://doi>
54
55
1045 [.org/10.1073/pnas.1317692111](https://doi.org/10.1073/pnas.1317692111).
56
57
58
59
60
61
62
63
64
65

- 1
2
3
4
1046 Claassen, M. 2008. A note on the biostratigraphic application of Permian plant fossils of the
5
6
1047 Normandien Formation (Beaufort Group, Northeastern Main Karoo Basin, South Africa.
8
9
1048 S. Afr. J. Geol. 11. 263-280.
10
11
1049 Cohen, K.M., Finney, S.C., Gibbard, P.L., Fan, J.-X. 2013. (updated v. 2022/10) The ICS
13
14
1050 International Chronostratigraphic Chart. Episodes. 36. 199-204.
15
16
1051 Cole, D., 2017. Comment on the paper “Palynological records of the Permian Ecca Group (South
18
19
1052 Africa): Utilizing climatic icehouse-greenhouse signals for cross basin correlations” by K.
20
21
1053 Ruckwied, A. Götz and P. Jones (PPP, 413, 167-172, 2014). Palaeo. Palaeo. Palaeo. 485.
23
24
1054 990–991.
25
26
1055 Cole, D., Barbolini, N. 2019. Marine flooding surfaces recorded in Permian black shales and coal
28
29
1056 deposits of the Main Karoo Basin (South Africa): Implications for basin dynamics and
30
31
1057 cross-basin correlation: Discussion. Int. J. Coal. Geol. 209. 130-131.
33
34
1058 <https://doi.org/10.1016/j.coal.2018.04.013>.
35
36
1059 Cole, D.I., Johnson, M.R., and Day, M.O. 2016. Lithostratigraphy of the Abrahamskraal
38
39
1060 Formation (Karoo Supergroup), South Africa. S. Afr. J. Geol. 119. 415–424. [https://doi](https://doi.org/10.2113/gssajg.119.2.415)
40
41
1061 [.org/10.2113/gssajg.119.2.415](https://doi.org/10.2113/gssajg.119.2.415).
43
44
1062 Davis, D.W., Rochín-Bañaga, H. 2021. A new Bayesian approach toward improved regression of
45
46
1063 low-count UPb geochronology data generated by LA-ICPMS. Chem. Geol. 582. 120454.
48
49
1064 <https://doi.org/10.1016/j.chemgeo.2021.120454>.
50
51
1065 Day, M. O., Ramezani, J., Bowring, S.A., Sadler, P.M., Erwin, D.H., Abdala, F, Rubidge, B.S.
53
54
1066 2015. When and how did the terrestrial mid-Permian mass extinction occur? Evidence
55
56
1067 from the tetrapod record of the Karoo Basin, South Africa. Proc. Roy. Soc. B.282.
58
59
60
61
62
63
64
65

1
2
3
4
5
6
7
8
9
10
11
12
13
14
15
16
17
18
19
20
21
22
23
24
25
26
27
28
29
30
31
32
33
34
35
36
37
38
39
40
41
42
43
44
45
46
47
48
49
50
51
52
53
54
55
56
57
58
59
60
61
62
63
64
65

20150834 . <https://doi.org/10.1098/rspb.2015.0834>

DiMichele, W.A., Gastaldo, R.A. 2008. Plant Paleocology in Deep Time. *Ann. Missouri Bot. Gard.* 95. 144-198.

Dunn, K.A., McLean, J.C., Upchurch, G., Folk, R.L. 1997. Enhancement of leaf fossilization potential by bacterial biofilms. *Geology*. 25. 1119–1122. DOI: 10.1130/0091-7613(1997)025<1119:EOLFPB>2.3.CO;2

Eshet, Y., Rampino, M.R., Visscher, H. 1995. Fungal event and palynological record of ecological crisis and recovery across the Permian-Triassic boundary: *Geology*. 23. 967–970. doi: [https://doi.org/10.1130/0091-7613\(1995\)023](https://doi.org/10.1130/0091-7613(1995)023)

Falcon, R.M.S. 1986. A brief review of the origin, formation and distribution of coal in Southern Africa. *In* Anhaeusser, C.R. Maske, S. Eds. *Mineral Deposits of Southern Africa*. *Geol. Soc. S. Afr.* 2. 1879–1898.

Falcon, R.M.S. 1989. Macro- and micro-factors affecting coal-seam quality and distribution in southern Africa with particular reference to the No. 2 seam, Witbank coalfield, South Africa. *Int. J. Coal Geol.* 12. 681-731. [https://doi.org/10.1016/0166-5162\(89\)90069-4](https://doi.org/10.1016/0166-5162(89)90069-4): 681731.

Fielding, C.R., Frank, T.D., McLoughlin, S., Vajda, V., Mays, C., Tevyaw, A.P., Winguth, A., Winguth, C., Nicoll, R.S., Bocking, M., Crowley, J.L. 2019. Age and pattern of the southern high-latitude continental end-Permian extinction constrained by multiproxy analysis. *Nature Comm.* 10. 385. doi: 10.1038/s41467-018-07934

Gastaldo, R.A. 1994. The genesis and sedimentation of phytoclasts with examples from coastal environments. *in* A. Traverse, ed. *Sedimentation of Organic Particles*. Cambridge

- 1
2
3
4
5 University Press. 103–127.
6
7
8
9
10
11
12
13
14
15
16
17
18
19
20
21
22
23
24
25
26
27
28
29
30
31
32
33
34
35
36
37
38
39
40
41
42
43
44
45
46
47
48
49
50
51
52
53
54
55
56
57
58
59
60
61
62
63
64
65
- University Press. 103–127.
- Gastaldo, R.A. Rolerson, M.W. 2008. *Katbergia* gen. nov., a new trace fossil from the Upper Permian and Lower Triassic Rocks of the Karoo Basin: Implications for paleoenvironmental conditions at the P/Tr extinction event. *Palaeontology*. 51. 215-229.
- Gastaldo, R.A., Demko, T.M. 2011. Long term hydrology controls the plant fossil record: *in* Allison, P.A., and Bottjer, D.J., eds., *Taphonomy, Second Edition: Processes and Bias Through Time: Topics in Geobiology*. 32. 249-286. (doi 10.1007/978-90-481-8643-3_7)
- Gastaldo, R.A., Staub, J.R. 1999. A mechanism to explain the preservation of leaf litter lenses in coals derived from raised mires. *Palaeo. Palaeo. Palaeo*. 149. 1-14.
- Gastaldo, R.A., Adendorff, R., Bamford, M.K., Labandeira, Neveling, J., Sims, H.J., 2005. Taphonomic trends of macrofloral assemblages across the Permian-Triassic Boundary, Karoo Basin, South Africa: *PALAIOS*. 20. 478-497. (doi 10.1016/j.palaeo.2010.03.052)
- Gastaldo, R.A., Knight, C., Neveling, J., Tabor, N. 2014. Late Permian paleosols from Wapadsberg Pass, South Africa: Implications for Changhsingian climate. *Geol. Soc. Am. Bull.* 126. 665-679: doi: 10.1130/B30887.1
- Gastaldo, R.A., Kamo, S.L., Neveling, J., Geissman, J., Bamford, M., Looy, C. 2015. Is the vertebrate-defined Permian–Triassic Boundary in the Karoo Basin, South Africa, the terrestrial expression of the End Permian marine event?. *GEOLOGY*. 43. 939-942.
- Gastaldo, R.A., Neveling, J., Looy, C., Bamford, M., Kamo, S.L., and Geissman, J.W. 2017. Paleontology of the Blaauwater Farm, South Africa: Testing the *Daptocephalus/Lystrosaurus* biozone boundary in a stratigraphic framework: *PALAIOS*. 34. 349-366. DOI: <http://dx.doi.org/10.2110/palo.2016.106>

- 1
2
3
4
5
6
7
8
9
10
11
12
13
14
15
16
17
18
19
20
21
22
23
24
25
26
27
28
29
30
31
32
33
34
35
36
37
38
39
40
41
42
43
44
45
46
47
48
49
50
51
52
53
54
55
56
57
58
59
60
61
62
63
64
65
- 1112 Gastaldo, R.A., Neveling, J., Geissman, J.W., Kamo, S.L. 2018a. A lithostratigraphic and
1113 magnetostratigraphic framework in a geochronologic context for a purported
1114 Permian–Triassic Boundary section at Old (West) Lootsberg Pass, Karoo Basin, South
1115 Africa. *Geol. Soc. Am. Bull.* 130. 1411-1438.
- 1116 Gastaldo, R.A., Looy, C., and Neveling, J., 2018b. Late Permian palynofloral assemblages from
1117 the *Daptocephalus* and *Lystrosaurus* assemblage zones, Karoo Basin, South Africa:
1118 taphonomic windows into climate oscillation: in McElwain, J., ed., EPPC 2018 10th
1119 European Palaeobotany and Palynology Conference, Dublin, Ireland, p. 110.
- 1120 Gastaldo, R.A., Neveling, J., Geissman, J.W., Li, J., 2019, A multidisciplinary approach to
1121 review the vertical and lateral facies relationships of the purported vertebrate-defined
1122 stratigraphic interval at Bethulie, Karoo Basin, South Africa: *Earth Sci. Rev.* 189. 220-
1123 243. doi: 10.1016/j.earscirev.2017.08.002.
- 1124 Gastaldo, R.A., Kamo, S.L., Neveling, J., Geissman, J., Looy, C.V., Martini, A.M. 2020a. The
1125 base of the *Lystrosaurus* Assemblage Zone, Karoo Basin, predates the end-Permian
1126 marine extinction: *Nat. Commun.* 11. 1428. <https://doi.org/10.1038/s41467-020-15243-7>
- 1127 Gastaldo, R.A., Kus, K., Neveling, J., Tabor, N. 2020b. Calcic paleoVertisols in the upper
1128 *Daptocephalus* Assemblage Zone, Balfour Formation, Karoo Basin, South Africa:
1129 Implications for Late Permian climate. *J. Sed. Res.* 90. 609-628. DOI:
1130 <http://dx.doi.org/10.2110/jsr.2020.32>
- 1131 Gastaldo, R.A., Tabor, N., Neveling, J., 2020c. Trends in Late Permian (Changhsingian)
1132 paleoclimate in the *Daptocephalus* Assemblage Zone, Eastern Cape Province, South
1133 Africa. *Front. Earth Sci.* 8. 567109. DOI:10.3389/fevo.2020.567109

- 1
2
3
4 134 Gastaldo, R.A., Wan, M., Yang, W. In press. The taphonomic character, occurrence, and
5
6
7 135 persistence of upper Permian–Lower Triassic plant assemblages in the
8
9 136 mid-paleolatitudes, Bogda Mountains, western China. *PALAIOS*
10
11
12 137 Götz, A.E., Hancox, P.J., Lloyd, A. 2017. Permian climate change recorded in palynomorph
13
14 138 assemblages of Mozambique (Moatize Basin, eastern Tete Province). *Acta Palaeobot.* 27.
15
16
17 139 3-11.
18
19 140 Groenewald, D.P., Day, M.O., Penn-Clarke, C.R., Rubidge, B.S. 2022. Stepping out across the
20
21
22 141 Karoo retro-foreland basin: Improved constraints on the Ecca-Beaufort shoreline along
23
24 142 the northern margin. *J. Afr. Earth Sci.* 185, 104389,
25
26
27 143 <https://doi.org/10.1016/j.jafrearsci.2021.104389>.
28
29 144 Hochuli, P., Sanson-Barrera, A., Schneebeli-Hermann, E., Bucher, H. 2016. Severest crisis
30
31
32 145 overlooked—Worst disruption of terrestrial environments postdates the Permian–Triassic
33
34 146 mass extinction. *Sci. Report.* 6. 10.1038/srep28372.
35
36
37 147 Holland, S.M., M.E. Patzkowsky. 2015. The stratigraphy of mass extinction. *Palaeontology*, 58,
38
39 148 903–924.
40
41
42 149 Hounslow, M.W., Balabanov, Y.P. 2016. A geomagnetic polarity time scale for the Permian,
43
44 150 calibrated to stage boundaries. *Geol. Soc. London Spec. Pub.* 450,
45
46
47 151 <https://doi.org/10.1144/SP450.8>.
48
49 152 Iniesto, M., Blanco-Moreno, C., Villalba, A., Buscalioni, Á.D., Guerrero, M.C., López-Archilla,
50
51
52 153 A.I. 2018. Plant tissue decay in long-term experiments with microbial mats. *Geosciences*.
53
54 154 8. 387. <https://doi.org/10.3390/geosciences8110387>
55
56
57 155 Johnson, M.R., Van Vuuren, C.J., Visser, J.N.J., Cole, D.I., Wickens, H. de V., Christie, A.D.M.,
58
59
60
61
62
63
64
65

1
2
3
4
5
6
7
8
9
10
11
12
13
14
15
16
17
18
19
20
21
22
23
24
25
26
27
28
29
30
31
32
33
34
35
36
37
38
39
40
41
42
43
44
45
46
47
48
49
50
51
52
53
54
55
56
57
58
59
60
61
62
63
64
65

Roberts, D.L., Brandl. G. 2006. Sedimentary rocks of the Karoo Supergroup. *In*: M.R. Johnson, C.R. Anhaeusser, R.J. Thomas, eds. The Geology of South Africa. Geological Society of South Africa, Johannesburg/Council for Geoscience, 461-501.

Katsiaficas, N., Gastaldo, R.A., Neveling, J. 2010. An analysis of geometric and sedimentologic characteristics of a Middle Permian fluvial system, Karoo Basin, South Africa. *Geol. Soc. Am. Abstr. with Progr.* 42. 174-20.

Kerp, H., Penati, F., Brambilla, G., Clement-Westerhof, J.A., van Bergen, P.F. 1996. Aspects of Permian palaeobotany and palynology. XVI. Three-dimensionally preserved stromatolite-incrusted conifers from the Permian of the western Orobic Alps (northern Italy). *Rev. Palaeobot. Palynol.* 91. 63-84.
[https://doi.org/10.1016/0034-6667\(95\)00065-8](https://doi.org/10.1016/0034-6667(95)00065-8).

Lacey, W.S. 1976. A review of the Upper Permian *Glossopteris* flora in western Natal. *Palaeobotanist.* 25. 185–189.

Lacey, W.S., van Dijk, D.E., Gordon-Gray, K.D. 1975. Fossil plants from the Upper Permian in the Mooi River district of Natal, South Africa. *Ann. Natal Mus.* 22. 349–420.

Locatelli, E. 2014. The exceptional preservation of plant fossils: a review of taphonomic pathways and biases in the fossil record. *Paleo. Soc. Pap.* 20. 237-258.
[doi:10.1017/S1089332600002874](https://doi.org/10.1017/S1089332600002874)

Looy C.V., Twitchett, R.J., Dilcher, D.L., Van Konijnenburg-Van Cittert, J.H., and Visscher, H., 2001, Life in the end-Permian dead zone: Proceedings of the National Academy of Science U S A., v. 98, p. 7879-7883. doi: 10.1073/pnas.131218098.

Lowrie, W. Kent, D.V., 2004. Geomagnetic Polarity Timescales and Reversal Frequency

1
2
3
4 178 Regimes. Geophys. Monogr. Ser. 145. 117-129. DOI: 10.1029/145GM09
5
6
7 179 Ludwig, K.R. 1998. On the treatment of concordant uranium-lead ages. Geochim. Cosmochim.
8
9 180 Acta. 62. 665-676.
10
11
12 181 MacRae, C.S., 1988. Palynostratigraphic correlation between the Lower Karoo sequence of the
13
14 182 Waterberg and Pafuri coal-bearing basins and the Hammanskraal plant macrofossil
15
16
17 183 locality, Republic of South Africa. Mem. Geol. Surv. S. Afr. 75. 1-217
18
19 184 Mahabeer, K.C. 2017. Palynology of the Permian Sanangoe-Mefidezi coal basin, Tete province,
20
21
22 185 Mozambique and correlations with Gondwana microfloral assemblages. Unpublished
23
24 186 M.Sc. Dissertation, University of the Witwatersrand, 168 p. URI:
25
26
27 187 <https://hdl.handle.net/10539/25813>
28
29 188 Marshall, J.E.A. 1990. Determination of thermal maturity. *In* Briggs, D.E.G. and Crowther, P.,
30
31
32 189 eds: Palaeobiology – a synthesis, 511–515. Blackwell Scientific Publications, Oxford,
33
34 190 UK.
35
36
37 191 Mays, C., McLoughlin, S. 2022. End-Permian Burnout: the role of Permian–Triassic wildfires in
38
39 192 extinction, carbon cycling, and environmental change in Eastern Gondwana. PALAIOS.
40
41
42 193 37. 292–317. doi: <https://doi.org/10.2110/palo.2021.051>
43
44 194 Mays, C., Vajda, V., Frank, T.D., Fielding, C.R., Nicoll, R.S., Tevyaw, A.P., McLoughlin, S.
45
46
47 195 2020. Refined Permian–Triassic floristic timeline reveals early collapse and delayed
48
49 196 recovery of south polar terrestrial ecosystems. Geol. Soc. Am. Bull. 132. 1489–1513. doi:
50
51
52 197 <https://doi.org/10.1130/B35355.1>
53
54 198 Mays, C., McLoughlin, S., Frank, T.D., Fielding, C.R., Slater, S.M., Vajda, V. 2021. Lethal
55
56
57 199 microbial blooms delayed freshwater ecosystem recovery following the end-Permian
58
59
60
61
62
63
64
65

- 1
2
3
4
1200 extinction. Nat. Commun. 12. 5511.
5
6
7
1201 McLoughlin, S., Prevec, R., Slater, B.J. 2021. Arthropod interactions with Permian *Glossopteris*
8
9
1202 flora. J. Palaeosci. 70. 43–133. 0031–0174/2021
10
11
1203 Nowak, H., Schneebeili-Hermann, E., Kustatscher, E. 2019. No mass extinction for land plants at
13
14
1204 the Permian–Triassic transition. Nat. Commun. 10, 1–8.
15
16
1205 Pace, D.W., Gastaldo, R.A., Neveling, J. 2009. Aggradational and degradational landscapes in
18
19
1206 the Early Triassic of the Karoo Basin and evidence for dramatic climate shifts following
20
21
1207 the P/Tr event. J. Sed. Res. 79. 276-291.
23
24
1208 Patzkowsky, M.E., Holland, S.M. 2012. Stratigraphic Paleobiology: Understanding the
25
26
1209 Distribution of Fossil Taxa in Time and Space. Chicago University Press, 256 p.
28
29
1210 Prevec, R., Labandeira, C.C., Neveling, J., Gastaldo, R.A., Looy, C.V., Bamford, M.K. 2009.
30
31
1211 Portrait of a Gondwanan ecosystem: A New Late Permian locality from Kwazulu-Natal,
33
34
1212 South Africa. Rev. Palaeobot. Palynol. 156. 454-493.
35
36
37
1213 Prevec, R., Gastaldo, R.A., Neveling, J., Reid, S.B., Looy, C.V. 2010. An autochthonous
38
39
1214 glossoperid flora with Latest Permian palynomorphs and its depositional setting from the
40
41
1215 *Dicynodon* Assemblage Zone of the southern Karoo Basin, South Africa: Palaeo. Palaeo.
43
44
1216 Palaeo. 292. 381-408. (doi: 10.1016/j.palaeo.2010.052)
45
46
47
1217 Retallack, G.G. 1988. Field recognition of paleosols. Geol. Soc. Am. Spec. Pap. 216. 1–19. DOI:
48
49
1218 10.1130/SPE216-p1
50
51
52
1219 Retallack, G.J., Smith, R.M.H., and Ward, P.D. 2003. Vertebrate extinction across the Permian–
53
54
1220 Triassic boundary in the Karoo Basin, South Africa. Geol. Soc. Am. Bull. 115.
55
56
1221 1133–1152.
58
59
60
61
62
63
64
65

- 1
2
3
4
1222 Roopnarine, P.D., Angielczyk, K.D., Weik, A., Dineen, A. 2019. Ecological persistence,
5
6
1223 incumbency and reorganization in the Karoo Basin during the Permian-Triassic
8
9
1224 transition: *Earth-Sci. Rev.* 189. 244-263. <https://doi.org/10.1016/j.earscirev.2018.10.014>.
10
11
1225 Rubidge, B. F., Hancox, J., Mason, R., 2012. Waterford Formation in the south-eastern Karoo:
13
14
1226 Implications for basin development. *S. Afr. J. Sci.* 108. 1-5. 10.4102/sajs.v108i3/4.829.
15
16
1227 Rubidge, B.S., Erwin, D.H., Ramezani, J., Bowring, S.A., de Klerk, W.J. 2013. High-precision
18
19
1228 temporal calibration of Late Permian vertebrate biostratigraphy: U-Pb zircon constraints
20
21
1229 from the Karoo Supergroup, South Africa. *GEOLOGY*. 41. 363-366.
23
24
1230 Ruckwied, K., Götz, A.E., Jones, P. 2014. Palynological records of the Permian Ecca Group
25
26
1231 (South Africa): Utilizing climatic icehouse–greenhouse signals for cross basin
28
29
1232 correlations. *Palaeo. Palaeo. Palaeo.* 413. 167–172.
30
31
1233 Schneebeili-Hermann, E. 2020. Regime shifts in an Early Triassic subtropical ecosystem. *Front.*
33
34
1234 *Earth Sci.* 8. 10.3389/feart.2020.588696.
35
36
1235 Schneebeili-Hermann, E., Hochuli, P.A., Bucher, H.F.R. 2017. Palynofloral associations before
38
39
1236 and after the Permian–Triassic mass extinction, Kap Stosch, East Greenland. *Global*
40
41
1237 *Planet. Change.* 155. DOI: 10.1016/j.gloplacha.2017.06.009
43
44
1238 Selover, R.W., Gastaldo, R.A. 2003. A reinterpretation of the Wagendrift Quarry, Estcourt,
45
46
1239 Kwazulu Natal Province, and its implications for Karoo Basin paleogeography. *Jour. S.*
48
49
1240 *Afr. Geol.* 108. 17-26.
50
51
1241 Sheldon, N.D., Tabor, N.J. 2009. Quantitative paleoenvironmental and paleoclimatic
53
54
1242 reconstruction using paleosols. *Earth-Sci. Rev.* 95. 1-52.
55
56
1243 Shen, S., Ramezani, J., Chen, J., Cao, C-Q., Erwin, D. H., Zhang, H., Xiang, L., Schoepfer, S.
58
59
60
61
62
63
64
65

- 1
2
3
4
1244 D., Henderson, C. M., Zheng, Q.-F., Bowring, S. A., Wang, Y., Li, X.-H., Yuan, D.-X.,
5
6
1245 Zhang, Y.-C., Mu, L., Wang, J., Wu, Y.-S., 2019, A sudden end-Permian mass extinction
8
9
1246 in South China. *Geol. Soc. Am. Bull.* 131. 205–223.
10
11
1247 Smith, R.M.H., 1995. Changing fluvial environments across the Permian-Triassic boundary in
13
14
1248 the Karoo basin, S.Africa and possible causes of tetrapod extinctions. *Palaeogr.*
15
16
1249 *Palaeoclim. Palaeoecol.* 117. 81–104. [https://doi.org/10.1016/0031-0182\(94\)00119-S](https://doi.org/10.1016/0031-0182(94)00119-S)
18
19
1250 Smith, R.M.H., Botha-Brink, J. 2014. Anatomy of a mass extinction: Sedimentological and
20
21
1251 taphonomic evidence for drought-induced die-offs at the Permo–Triassic boundary in the
23
24
1252 main Karoo Basin, South Africa. *Palaeogeogr. Palaeoclimat. Palaeoecol.* 396. 99–118.
25
26
1253 <https://doi.org/10.1016/j.palaeo.2014.01.002>.
28
29
1254 Smith, R.M.H., Ward, P.D. 2001. Pattern of vertebrate extinctions across an event bed at the
30
31
1255 Permian–Triassic boundary in the Karoo Basin of South Africa. *Geology.* 29. 1147–1150.
33
34
1256 [https://doi.org/10.1130/0091-7613\(2001\)029](https://doi.org/10.1130/0091-7613(2001)029)
35
36
1257 Smith, R.M.H., Rubidge, B.S., Day, M.O., Botha, J. 2020. Introduction to the tetrapod
38
39
1258 biozonation of the Karoo Supergroup. *S. Afr. J. Geol.* 123. 131-140.
40
41
1259 [doi:https://doi-org.colby.idm.oclc.org/10.25131/sajg.123.0009](https://doi-org.colby.idm.oclc.org/10.25131/sajg.123.0009)
43
44
1260 Smith, R.M.H., Botha, J., and Viglietti, P.A., 2022, Taphonomy of drought afflicted tetrapods in
45
46
1261 the Early Triassic Karoo Basin, South Africa: *Palaeogeography, Palaeoclimatology,*
48
49
1262 *Palaeoecology*, v. 604, 111207, <https://doi.org/10.1016/j.palaeo.2022.111207>.
50
51
1263 Steiner, M.B., Eshet, Y., Rampino, M.R., Schwindt, D.M. 2003. Fungal abundance spike and the
53
54
1264 Permian–Triassic boundary in the Karoo Supergroup (South Africa). *Palaeo. Palaeo.*
55
56
1265 *Palaeo.* 194. 405–414.
58
59
60
61
62
63
64
65

- 1
2
3
4
1266 Svensen, H., Corfu, F., Polteau, S., Hammer, Ø., Planke, S., 2012. Rapid magma emplacement in
5
6
1267 the Karoo Large Igneous Province. *Earth Planet. Sci. Lett.* 325–326. 1–9.
8
9
1268 <http://dx.doi.org/10.1016/j.epsl.2012.01.015>.
10
11
1269 Utting, J., Hamblin, A.P. 1991. Thermal maturity of the Lower Carboniferous Horton Group,
13
14
1270 Nova Scotia. *Int. J. Coal Geol.* 13. 439–456.
15
16
1271 Vajda, V., McLoughlin S., Mays, C., Frank, T.D., Fielding, C.R., Tevyaw, A., Lehsten, V.,
18
19
1272 Bocking, M., and Nicoll, R.A. 2020. End-Permian (252 Mya) deforestation, wildfires and
20
21
1273 flooding—An ancient biotic crisis with lessons for the present. *Earth Planet. Sci. Lett.*
23
24
1274 529. 115875
25
26
1275 Viglietti, P.A. 2020. Biostratigraphy of the *Daptocephalus* Assemblage Zone (Beaufort Group,
28
29
1276 Karoo Supergroup), South Africa. *S. Afr. J. Geol.* 123.2. 191-206.
30
31
1277 [doi:10.25131/sajg.123.0014](https://doi.org/10.25131/sajg.123.0014)
33
34
1278 Viglietti, P.A., Smith, R.M.H., Compton, J.S. 2013. Origin and palaeoenvironmental significance
35
36
1279 of *Lystrosaurus* bonebeds in the earliest Triassic Karoo Basin, South Africa. *Palaeog.*
38
39
1280 *Palaeoclim. Palaeoecol.* 392. 9-21. <https://doi.org/10.1016/j.palaeo.2013.08.015>.
40
41
1281 Viglietti, P.A., Rubidge, B.S., Smith, R.M.H. 2017. New Late Permian tectonic model for South
43
44
1282 Africa's Karoo Basin: foreland tectonics and climate change before the end-Permian
45
46
1283 crisis. *Sci Rep.* 7. 10861. doi: 10.1038/s41598-017-09853-3.
48
49
1284 Viglietti, P.A., Benson, R.B.J., Smith, R.M.H., Botha, J., Kammerer, C.F., Skosan, Z., Butler, E.,
50
51
1285 Crean, A., Eloff, B., Kaal, S., Mohoi, J., Molehe, W., Mtalana, N., Mtungata, S., Ntheri,
53
54
1286 N., Ntsala, T., Nyaphuli, J., October, P., Skinner, G., Strong, M., Stummer, H.,
55
56
1287 Wolvaardt, F.P., Angielczyk, K.D. 2021. Evidence from South Africa for a protracted
58
59
60
61
62
63
64
65

1
2
3
4
5
6
7
8
9
10
11
12
13
14
15
16
17
18
19
20
21
22
23
24
25
26
27
28
29
30
31
32
33
34
35
36
37
38
39
40
41
42
43
44
45
46
47
48
49
50
51
52
53
54
55
56
57
58
59
60
61
62
63
64
65

end-Permian extinction on land: Proc. Nat. Acad. Sci. USA. 118, e2017045118.
<https://doi:10.1073/pnas.2017045118>

Viglietti, P.A., Rojas, A., Rosvall, M., Klimes, B., Angielczyk, K.D. 2022. Network-based biostratigraphy for the late Permian to mid-Triassic Beaufort Group (Karoo Supergroup) in South Africa enhances biozone applicability and stratigraphic correlation. *Palaeontology*. 65. e12622. <https://doi.org/10.1111/pala.12622>

Wagner, N., Eble, C., Hower, J., Falcon, R. 2019. Petrology and palynology of select coal samples from the Permian Waterberg Coalfield, South Africa. *Int. J. Coal Geol.* 204. 85-101.

Wall, P.D., Ivany, L.C., Wilkinson, B.H. 2009. Revisiting Raup: Exploring the influence of outcrop area on diversity in light of modern sample-standardization techniques: *Paleobiol.* 35. 146–167.

Wall, P.D., Ivany, L.C., Wilkinson, B.H. 2011. Impact of outcrop area on estimates of Phanerozoic terrestrial biodiversity trends: *in* McGowan, A.J., and Smith, A.B., eds., *Comparing the Geological and Fossil Records: Implications for Biodiversity Studies: Geol. Soc. London Spec. Pub.* 358. 53–62.

Ward, P.D., Montgomery, D.R., Smith, R.M.H. 2000. Altered river morphology in South Africa related to the Permian–Triassic extinction. *Science*, 289. 1740–1743.

Ward, P.D., Botha, J., Buick, R., Dekock, M.O., Erwin, D.H., Garrison, G., Kirschvink, J., Smith, R.M.H. 2005. Abrupt and gradual extinction among Late Permian land vertebrates in the Karoo Basin, South Africa. *Science*, 307. 709–714.

Zavada, M.A., Mentis, M.T. 1992. Plant-animal Interaction: The Effect of Permian

1
2
3
4
5
6
7
8
9
10
11
12
13
14
15
16
17
18
19
20
21
22
23
24
25
26
27
28
29
30
31
32
33
34
35
36
37
38
39
40
41
42
43
44
45
46
47
48
49
50
51
52
53
54
55
56
57
58
59
60
61
62
63
64
65

megaherbivores on the Glossopterid flora. *Am. Midl. Nat.* 127. 1-12.

Table Captions

TABLE 1 – The stratigraphic position of Eastern Cape and Free State province localities used in the current compilation noting: the number of measured sections and their total stratigraphic thickness; the number of intervals from which permineralized wood, megafloras, and microfloras have been either reported or observed; and references for published fossil-plant assemblages.

Note that data on measured sections published by earlier workers are not included because of uncertainty about where mega- or microfloras were recovered. ¹Thickness of measured sections is based only on work of the authors and colleagues unless specified. ²The number of sections and total thickness of rock measured on Bethel farm includes both Palingkloof and Katberg intervals (see discussion in Gastaldo et al., 2019 for problems in the placement for the base of the Katberg Formation). ³Tweefontain consists of three dongas geographically separated over a lateral distance of 4.5 km (See Gastaldo et al., 2021).

Table 2 – Number of horizons and percentage of stratigraphic record from which permineralized wood, adpression megafloras, paleosols with subaerial litters and subsurface rooting have been recovered, and productive-and-figured palynological assemblages per locality (see Table 1). In addition, numbers of individual samples from which palynological assemblages have been reported in the literature are separated.

Figure Captions

Figure 1. Map of the main Karoo Basin, South Africa, showing the geographical distribution of the Dwyka and Ecca Groups (Carboniferous–Permian), the Permian-and-Triassic vertebrate biozones and the Jurassic Drakensberg Group. Vertebrate Assemblage Zones follow Smith et al.

1
2
3
4
5
6
7
8
9
10
11
12
13
14
15
16
17
18
19
20
21
22
23
24
25
26
27
28
29
30
31
32
33
34
35
36
37
38
39
40
41
42
43
44
45
46
47
48
49
50
51
52
53
54
55
56
57
58
59
60
61
62
63
64
65

(2020) with the exception of the *Daptocephalus* and *Lystrosaurus* Assemblage Zones as demonstrated to be coeval by Gastaldo et al. (2021).

Figure 2. Generalized stratigraphy of the continental Beaufort Group and lithostratigraphic subdivision east of 24° longitude as recognized by the South African Committee on Stratigraphy (Johnson et al., 2006; Cole et al., 2016). Magnetostratigraphy of the Beaufort Group from Gastaldo et al. (2017, 2018, 2019, 2020a, 2021). U-Pb ages are from ¹Rubidge et al. (2013), ²Gastaldo et al. (2015), ³Gastaldo et al. (2020a), and ⁴unpublished (white arrow). The biostratigraphic overlap of the Last Appearance Datum of the diagnostic taxa used to define the *Daptocephalus* Assemblage Zone and First Appearance Datum of the diagnostic taxa used to define the base of the *Lystrosaurus declivis* AZ are depicted. The stratigraphic range of the *Dulhuntyispora parvithola* (Changhsingian), *Playfordiaspora crenulata* (Changhsingian–Induan) and *Protohaploxypinus microcorpus* (Induan) palynozones are shown. The placement of the Permian–Triassic boundary in the Katberg Formation follows Gastaldo et al. (2021).

Figure 3. Maps of classic localities where the Permian–Triassic transition and boundary (PTB) are reported in the literature. (A) Eastern Cape Province localities reviewed in this manuscript with generalized GPS (WGS84 standard) coordinates. (B) Free State localities reviewed in this manuscript with generalized GPS (WGS84 standard) coordinates. See text for details.

Figure 4. Characteristic megafloreal elements of the Beaufort Group. (A) Leaf mat of randomly oriented, mineralized impressions of *Glossopteris* leaves, Onder Karoo, Northern Cape Province. (B) Leaf mat of randomly oriented, mineralized impressions of *Glossopteris* leaves preserved in an abandoned channel deposit, Clouston farm, KwaZulu Natal Province (Prevec et al., 2009). (C) Equisetalean dominated assemblage of isolated whorls of *Phyllothea* (Ph), axes with whorled

1
2
3
4
5 1354 leaves assigned to *Tryzigia* (Tr), and associated three-dimensionally preserved reproductive
6
7 1355 strobili (Str), Old Wapadsberg Pass, Eastern Cape Province. Scales in mm and cm.
8
9
10 1356 Figure 5. *Glossopteris* herbivory. (A) Feeding holes penetrating *Glossopteris* morphotype W1 of
11
12 1357 Prevec et al. (2010). (B) Surface feeding. (C) Deeply incised margin feeding. (D) Leaf mining.
13
14 1358 Wapadsberg Pass, Eastern Cape Province. Scale in mm and cm.
15
16
17 1359 Figure 6. Megafloral elements reported by Retallack et al. (2003, p. 1147) from Carlton Heights.
18
19 1360 Collection sent to the first author along with letter with identifications, currently curated in the
20
21
22 1361 Paleobotanical collection of the Evolutionary Studies Institute, Johannesburg. (A) *Lepidopteris*,
23
24 1362 Retallack collection number 4643; (B) *Lepidopteris*, Retallack collection number 4635; (C)
25
26 1363 *Pagiophyllum*, Retallack collection number 4645; (D) *Pagiophyllum*, Retallack collection
27
28 1364 number 4637; (E) *Cladophlebis*, Retallack collection number 4664; (F) *Samaropsis*, Retallack
29
30 1365 collection number 4646. Scales in mm.
31
32
33
34 1366 Figure 7. Karoo Fossil Wood, where generic identification is best discriminated in Radial
35
36
37 1367 Longitudinal Section (RLS). Anatomical features in neither Transverse (TS) nor Transverse
38
39 1368 Longitudinal (TLS) section are useful for generic identification. (A) TS of a typical Permian
40
41 1369 pycnoxylic gymnosperm wood with uniform rows of round to square tracheids. Magnification
42
43 1370 40x. (B) TLS of a typical Permian pycnoxylic gymnosperm wood with longitudinal tracheids and
44
45 1371 uniseriate, homocellular rays (R). (C) RLS of Early Permian *Prototaxoxylon uniseriale* with
46
47 1372 spiral thickenings on the tracheids. Bordered pits (bp) are uniseriate and cross-field pits (cf) are
48
49 1373 cupressoid or taxodioid. (D) RLS of *Australoxylon teixeirae* (Permian) with clusters of borders
50
51 1374 pits on the tracheid walls. (E) RLS of *Agathoxylon africanum*, the most common woody
52
53 1375 spanning late Permian–Triassic, with biseriate alternate bordered pitting. (F) RLS of late Permian
54
55
56
57
58
59
60
61
62
63
64
65

1
2
3
4
1376 *Agathoxylon karooensis* with bi-to-triseriate alternate bordered pitting. Scale: all tracheids are
5
6
1377 35-40 µm in diameter.
8
9
1378 Figure 8. Representative Beaufort Group palynomorphs. Algae: (A) *Mehlisphaeridium* sp.,
10
11
1379 Quaggasfontein farm, Eastern Cape. Equisetales: (B) *Calamospora* sp., Quaggasfontein farm,
13
14
1380 Eastern Cape; (C) *Columinsiporites* cf. *peppersii*, Wapadsberg Pass, Eastern Cape (Prevec et al.,
15
16
1381 2010; UCMP 398617, SA-NWP2.A, E37-1). Pteridophytales: (D) *Horriditriletes teretangulatus*,
18
19
1382 Clouston Farm, Kwazulu Natal (Prevec et al., 2009; UCMP 398623, SA-CA0.5-9, H37-4.).
20
21
1383 Glossopteridales: (E) *Protohaploxylinus* sp., (F) *Striatiopodocarpites* sp., Quaggasfontein farm,
23
24
1384 Eastern Cape, (G) *Striatiopodocarpites cancellatus*, Clouston Farm, Kwazulu Natal (Prevec et
25
26
1385 al., 2009; UCMP 398628, SA-CA0.5-5, C44-3); Peltaspermales and Voltziales: (H)
28
29
1386 *Scheuringipollenites* sp., (I) *Alisporites* sp., Quaggasfontein farm, Eastern Cape; Voltziales: (J)
30
31
1387 *Guttulapollenites* sp., Quaggasfontein farm, Eastern Cape. Gymnospermales (?Peltaspermales):
33
34
1388 (K) *Falcisporites australis*, Quaggasfontein farm, Eastern Cape. Fungal/algal: (L)
35
36
1389 *Reduviasporonites* sp., Donald 207 farm (Gastaldo et al., 2019; UCMP PA1351.1, 398664,
38
39
1390 M49-1). Note range of palynomorph color, ranging from yellow-brown (~100° C; thermal
40
41
1391 alteration index 2; Utting and Hamblin 1991) to black (>200° C, thermal alteration index 4+), as
43
44
1392 a function of post-depositional thermal alteration in response to the emplacement of the Karoo-
45
46
1393 Ferrar dolorites. Taxonomic names are followed by a UCMP collection locality number code, the
48
49
1394 UCMP specimen number, and England Finder graticule coordinates. Scale = 50 µm. Images
50
51
1395 courtesy of C.V. Looy.

52
53
54
1396 Figure 9. Cryptic reverse polarity magnetozone exposed beneath an erosional unconformity (S
55
56
1397 31.795125°, E 024.798815°) at Old Lootsberg Pass, Blaauwater farm (Gastaldo et al., 2018).
58
59

1
2
3
4 1398 The landscape was reset by the erosion of sediments deposited during a reverse-polarity chron
5
6 1399 with the emplacement of a 11-m thick fluvial deposit at the onset of a degradational phase in this
7
8
9 1400 part of the basin. Sampled anywhere else, the presence of a subjacent and suprajacent normal
10
11 1401 polarity magnetozone in contact with each other would evidence an impression of a continuous
12
13
14 1402 time interval over which these sediments accumulated. The presence of a reverse polarity
15
16 1403 magnetozone, though, demonstrates a significant temporal hiatus in the stratigraphic record.
17
18
19 1404 Borehole sample sites are evident in the walls of the donga; scale in decimeters.
20
21
22 1405 Figure 10. A modified Wheeler diagram in which four correlated stratigraphic sections over a 5.5
23
24 1406 km distance along the escarpment from Old Lootsberg Pass to Lootsberg Pass (Gastaldo et al.,
25
26 1407 2018, 2021) are shown in time-equivalent units. Time-equivalent units are bounded at the base
27
28
29 1408 by either: (1) an intraformational pedogenic lag deposit of a fluvial channel, the contact with the
30
31 1409 underlying lithology represents an erosional unconformity that signals a phase of landscape
32
33
34 1410 degradation; or (2) the identification of a non-conforming magnetozone between the subjacent
35
36 1411 and suprajacent lithologies indicating significant missing time at the contact. U-Pb CA-ID-TIMS
37
38
39 1412 ages constrain time, beds in which fossil plants are preserved are identified, and the position of
40
41 1413 diagnostic vertebrates used to separate the *Daptocephalus* AZ from the overlying *L. declivis* AZ
42
43
44 1414 as reported in the literature (Viglietti, 2020; Botha and Smith, 2020). Magnetostratigraphy shown
45
46 1415 for Old Lootsberg Pass and Tweefontein² sections (Gastaldo et al., 2021). Note the absence of
47
48
49 1416 any evidence of reverse polarity magnetozones in most sections, which is a function of either
50
51 1417 erosion or logistical sampling of incompetent lithologies. GPS coordinates (WGS84 standard) are
52
53
54 1418 presented for the top of measured sections; see Gastaldo et al. (2018, 2021) for detailed sections
55
56 1419 and their correlation across Blaauwater–Tweefontein–Lootsberg Pass.
57
58
59
60
61
62
63
64
65

1
2
3
4
5
6
7
8
9
10
11
12
13
14
15
16
17
18
19
20
21
22
23
24
25
26
27
28
29
30
31
32
33
34
35
36
37
38
39
40
41
42
43
44
45
46
47
48
49
50
51
52
53
54
55
56
57
58
59
60
61
62
63
64
65

Figure 11. Summary diagram of *Glossopteris*-dominated and palynological assemblages in geochronometric and magnetostratigraphic context reported from classic Karoo localities in which the Permian–Triassic boundary is reported by various workers. Palynozones, their current age assignments, and age ranges as reported in Eastern Australia (Mays and McLoughlin, 2022) are illustrated against a composite section for the Karoo Basin. South African Provinces: EC = Eastern Cape; FS = Free State. Localities: BW = Blaauwater farm, Old Lootsberg Pass; TW¹ = Tweefontein¹, TW² = Tweefontein², WP = Wapadsberg Pass; NT = Nooitgedacht; D207 = Donald 207 farm. Gray bar indicates that no rock magnetic data are available for this part of the composite section; text of preliminary, unpublished U-Pb age estimate appears in gray.

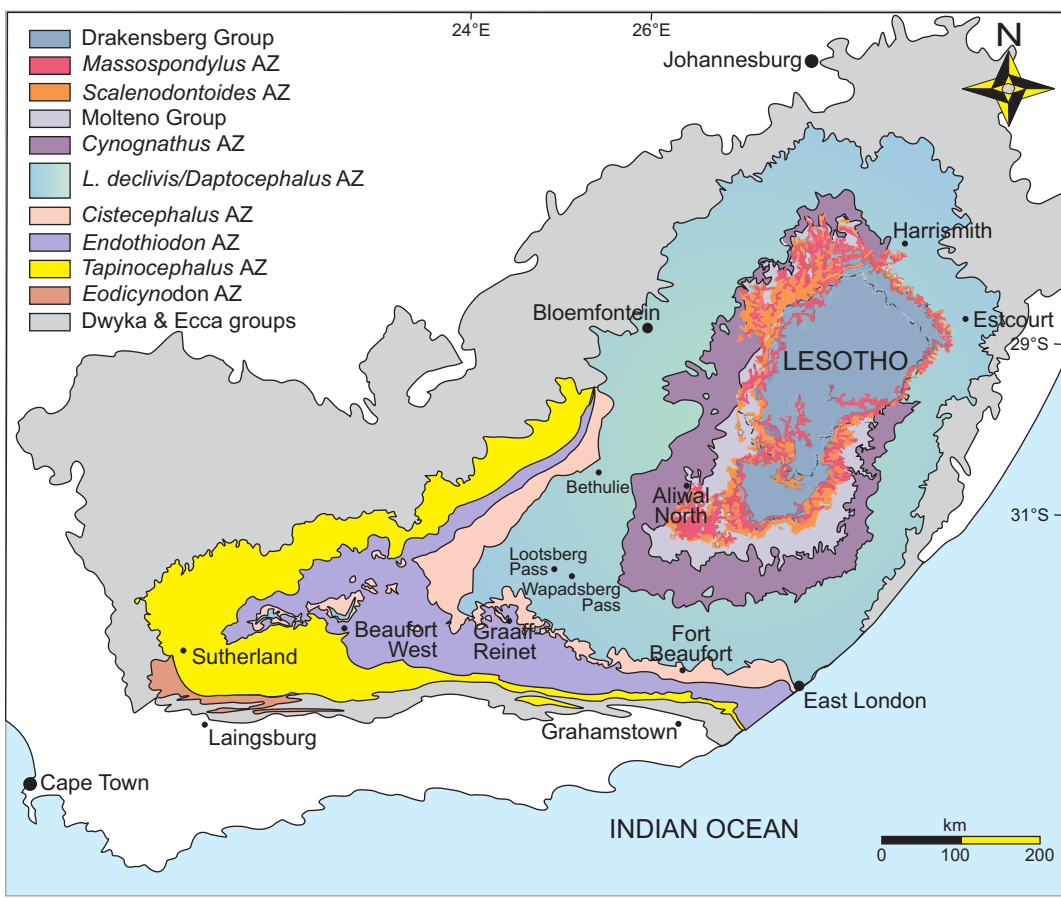
Period	Stratigraphic Unit	Locality	# Measured Sections ¹	Total Thickness ¹	Permin. Wood	Adpression Macroflora	Palynoflora	Citation	
Triassic	Burgersdorp Fm.	Boesmanshoek	1	75 m		1		Gastaldo et al. (2005)	
	Katberg Fm.	Carlton Heights					22 ⁴	Steiner et al. (2003)	
Upper Permian		Carlton Heights				1		Retallack et al. (2003)	
		Carlton Heights	8	380 m		1		Gastaldo et al. (2005); Pace et al. (2009)	
		Balfour Fm.							
		Palingkloof Mbr	Carlton Heights	1	60 m		1		Gastaldo et al. (2005); unpublished
			Nooitgedacht	2	86 m		5		Botha et al. (2020)
			Nooitgedacht	1	70 m			2	Gastaldo et al. (2020)
			Donald 207 / Fairydale	8	340 m			1	Barbolini et al. (2018) Gastaldo et al. (2019)
			Bethel / Heldenmoed farm ²	13	685 m		2		Gastaldo et al. (2005, 2009, 2019, 2020)
			CommandoDrift	2	210 m		2	12 ⁴	Gastaldo et al. (2005); unpublished Coney et al., (2007)
			Old Lootsberg Pass (Blaauwater)	13	880 m	2	6	1	Gastaldo et al. (2017)
			Tweefontein ³	7	780 m				Gastaldo et al. (2017, 2021)
			Lootsberg Pass	3					Gastaldo et al. (2021); unpublished
			Pienaarsbaaken	2	180 m		1	1	unpublished
			Quaggasfontein	1	155 m	1	4	3	Gastaldo et al. (2020)
			Quaggasfontein					2	Gastaldo et al. (2018); unpublished
			Old Wapadsburg Pass/ Pienaarsbaaken	8	730 m	1	2	3	Gastaldo et al. (2005); Prevec et al. (2010)
		New Wapadsburg Pass	1	65 m		2	1	Gastaldo et al. (2014, 2018); Prevec et al. (2010); unpublished	
	Elandsberg Mbr. ?	Tweefontein				1	1	Gastaldo et al. (2017)	

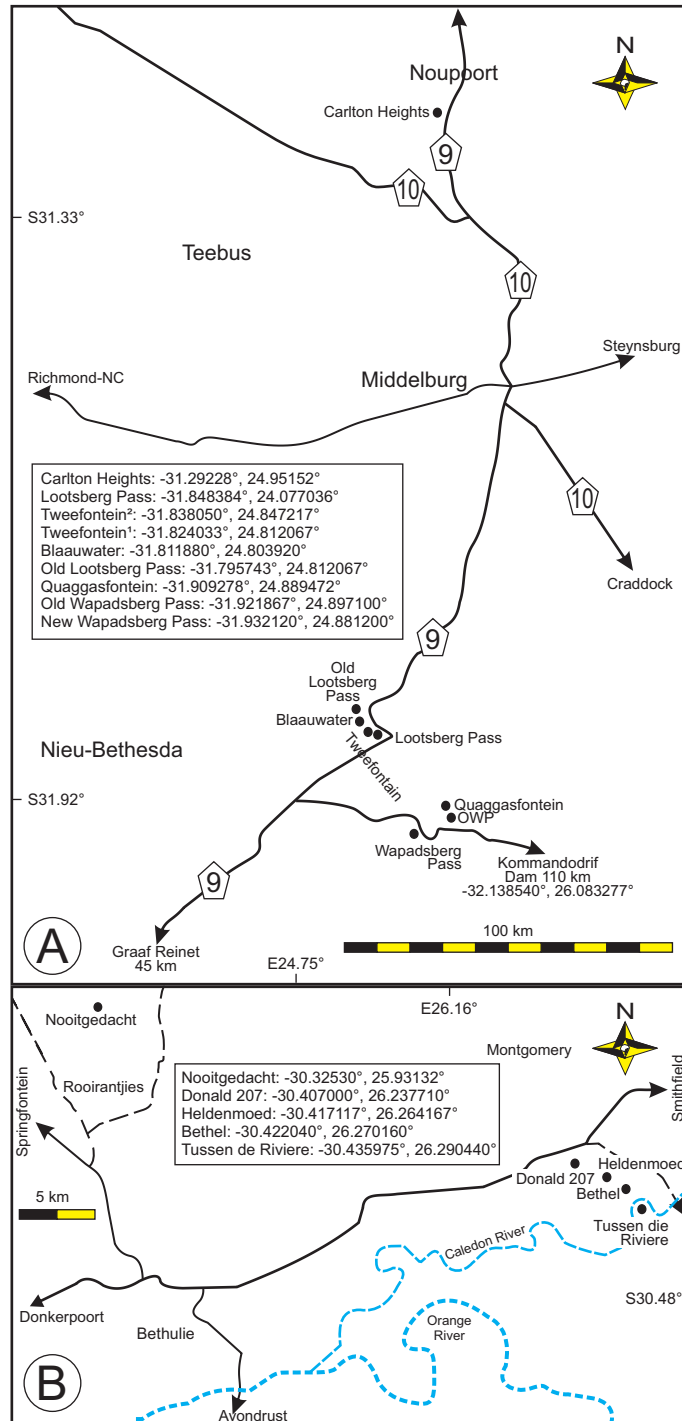
TABLE 1 – The stratigraphic position of Eastern Cape and Free State province localities used in the current compilation noting: the number of measured sections and their total stratigraphic thickness; the number of intervals from which permineralized wood, macrofloras, and microfloras have been either reported or observed; and references for published fossil-plant assemblages. Note that measured sections published by earlier workers have not been included because their is uncertainty about where mega- or microfloras were recovered. ¹ Thickness of measured sections is based only

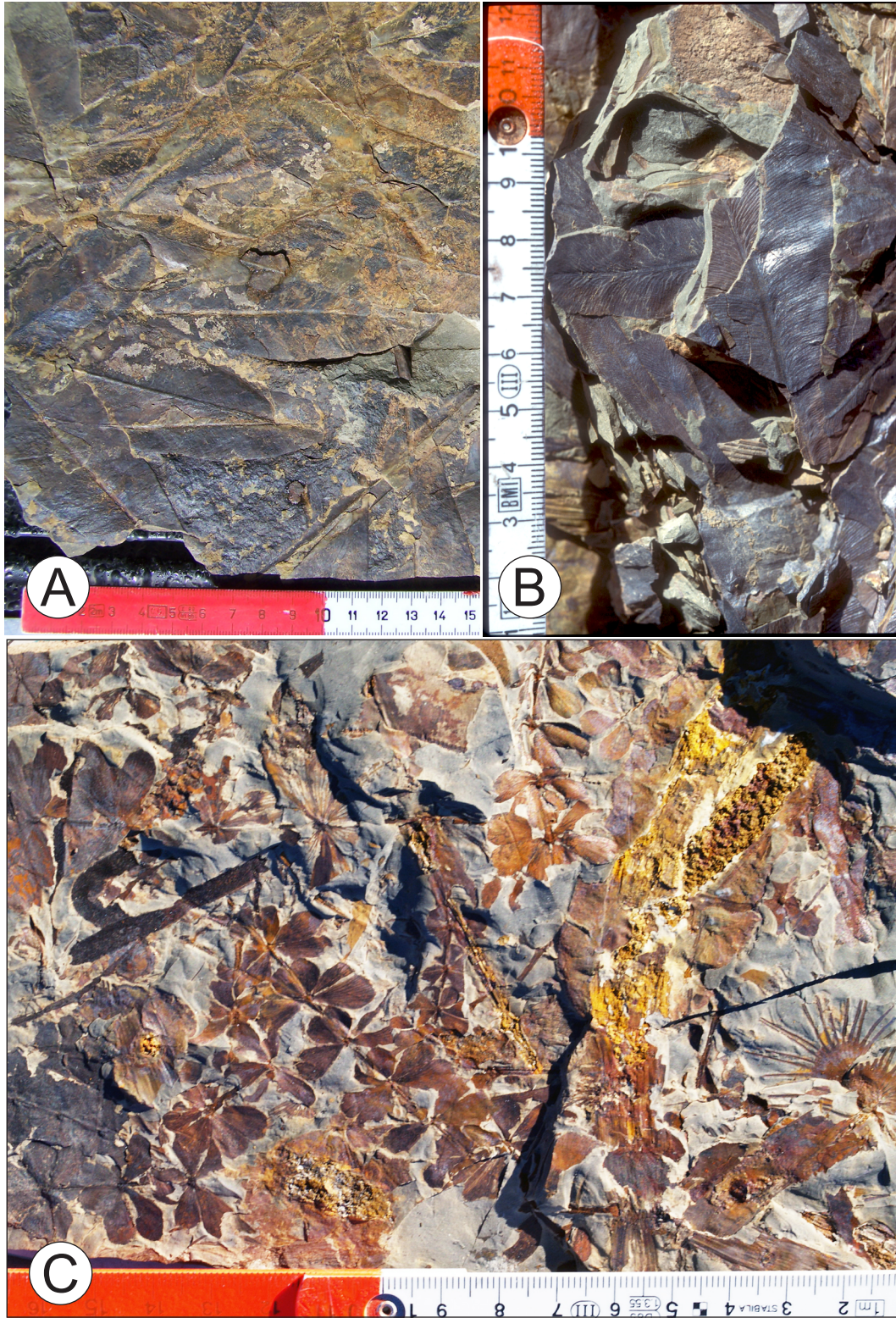
on work of the authors and colleagues unless specified. ² The number of sections and total thickness of rock measured on Bethel and Heldenmoed farms includes both Palingkloof and Katberg intervals (see discussion in Gastaldo et al., 2019 for problems in the placement for the base of the Katberg Formation). ³ Tweefontain consists of three dongas geographically separated over a lateral distance of 4.5 km (See Gastaldo et al., 2021). ⁴ Number of productive samples reported in the literature; our palynology values indicate productive localities or stratigraphic intervals rather than number of productive samples.

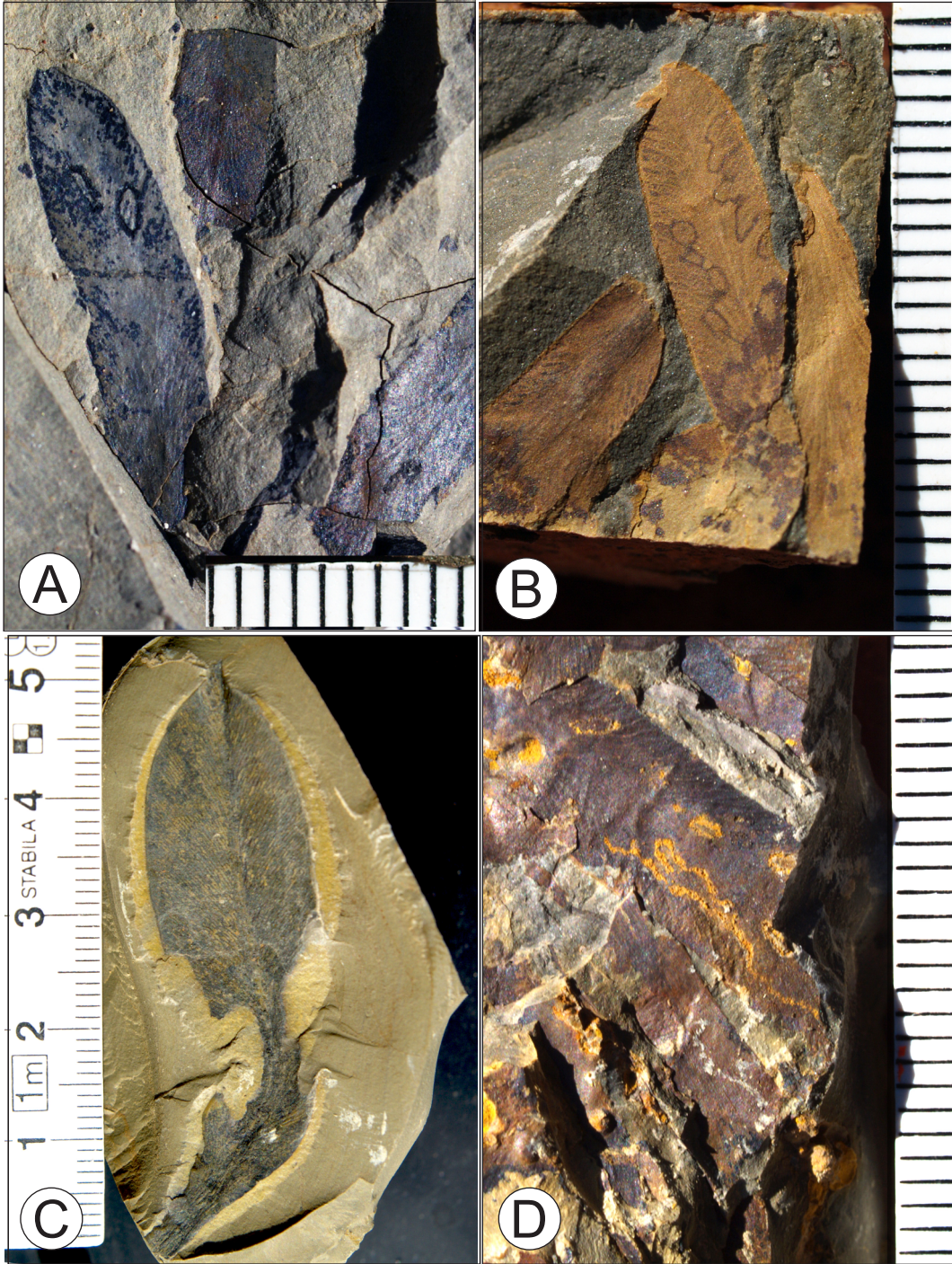
Total Meters of Measured Section	Permineralized Wood	Adpression assemblages	Paleosols w/adpression leaf litters and rooting	Palynology
3960	4	28	1	16
	0.10%	0.71%	0.03%	0.40%
Microfloras from literature				48
				1.3%

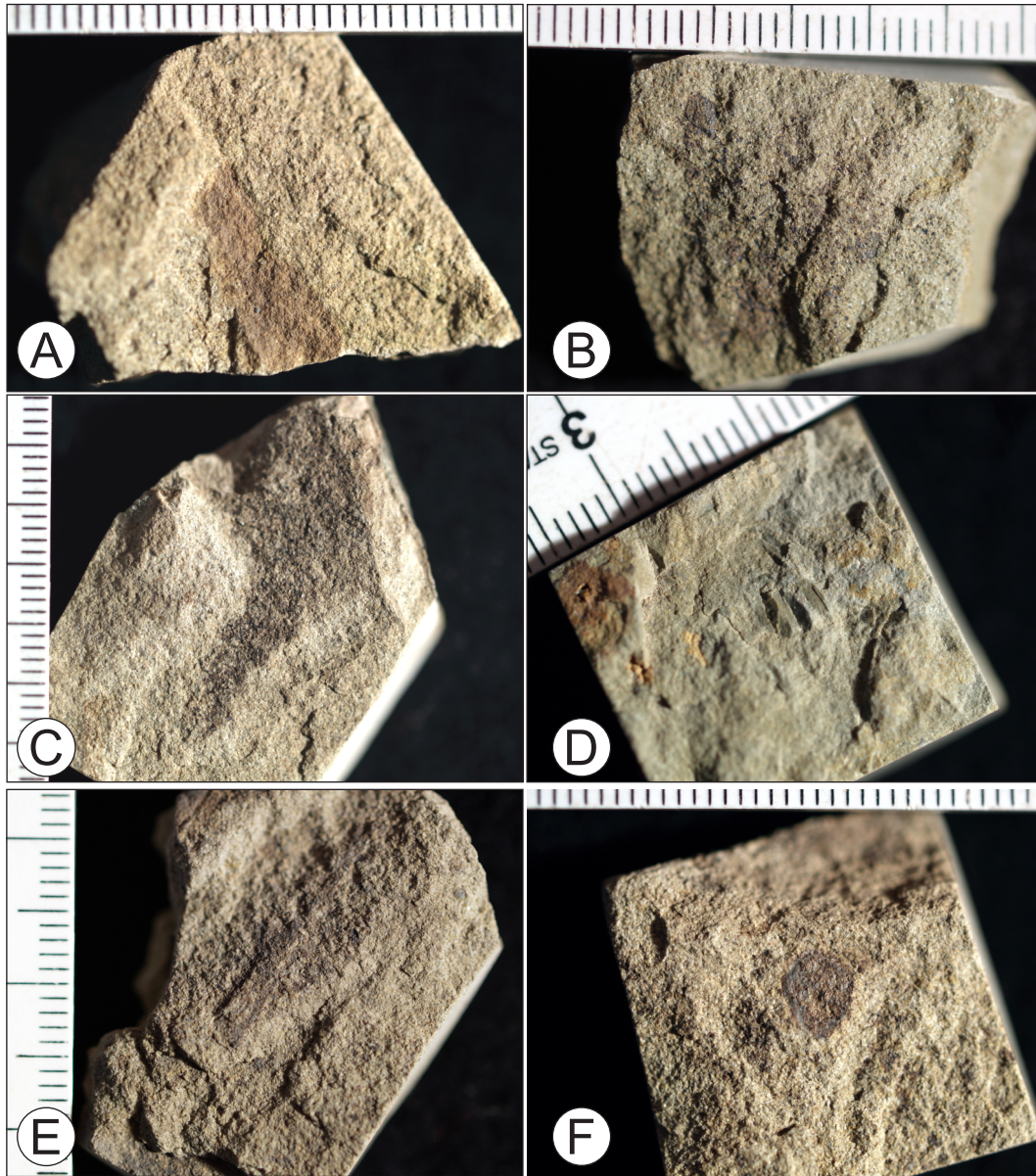
TABLE 2 - Number of horizons and percentage of stratigraphic record from which permineralized wood has been recovered, adpression megafloras, paleosols with subaerial litters and subsurface rooting, and productive and figured palynological assemblages per locality in our database (see Table 1). In addition, numbers of individual samples from which palynological assemblages have been reported in the literature are separated. The value assumes that each fossil assemblage is preserved over a 1 m interval of rock; in reality, most are found over a few centimeters to decimeters of rock.

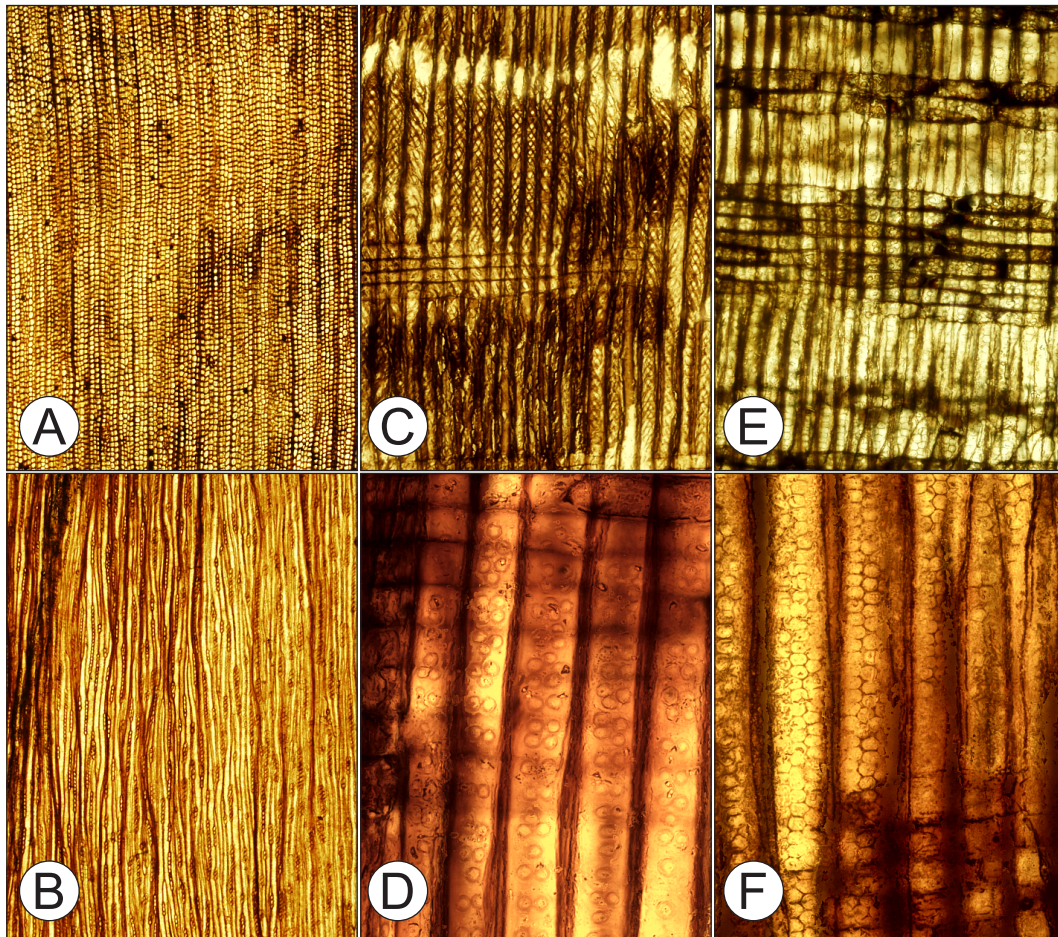


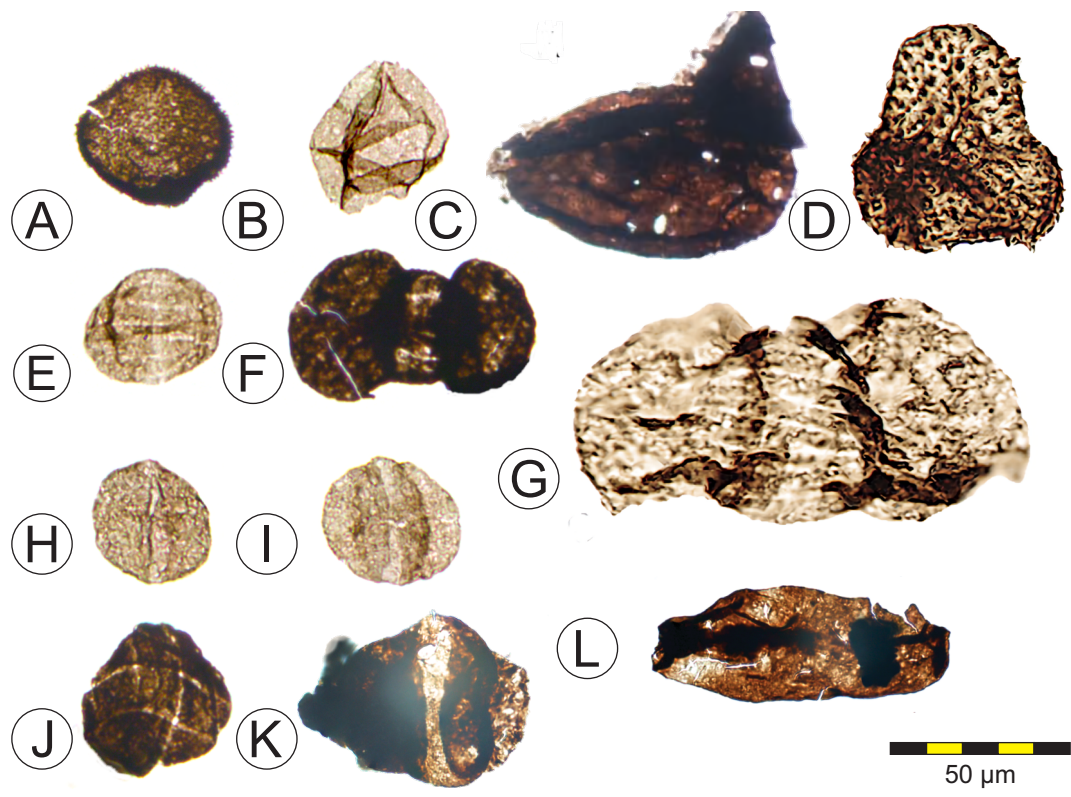




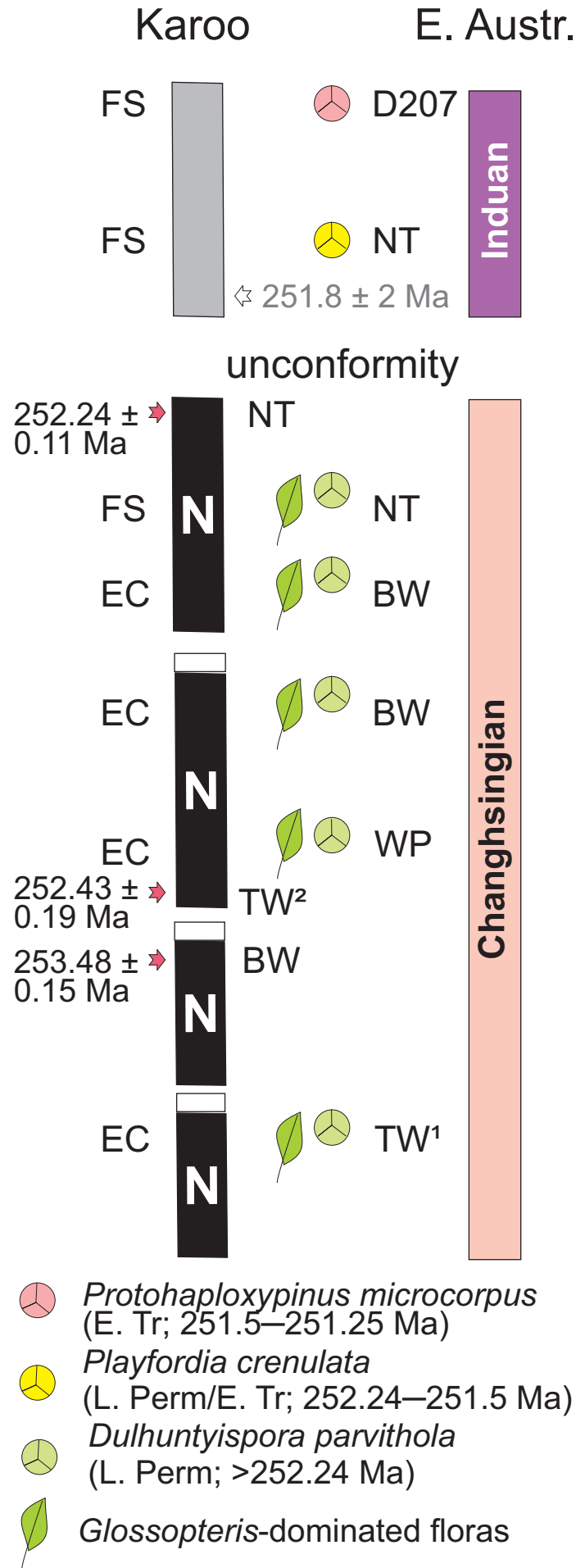












The influence of taphonomy and time on the paleobotanical record of the Permian–Triassic transition of the Karoo Basin (and elsewhere)

Robert A. Gastaldo¹

Department of Geology, Colby College, Waterville, ME 04901 USA

and

Marion K. Bamford

Evolutionary Studies Institute, University of Witwatersrand, 1 Jan Smuts Avenue, Braamfontein
2000, Johannesburg, South Africa

¹Corresponding Author email: ragastal@colby.edu

Declaration of interests

The authors declare that they have no known competing financial interests or personal relationships that could have appeared to influence the work reported in this paper.

The authors declare the following financial interests/personal relationships which may be considered as potential competing interests: